Electroweak Physics at the EIC

Sonny Mantry
University of North Georgia (UNG)

Uncovering New Laws of Nature at the EIC
Brookhaven National Laboratory
November 20th-22nd, 2024

Parity-Violating Electron-Deuteron Asymmetry

$$A_{PV} = \frac{\sigma_R - \sigma_L}{\sigma_R + \sigma_L}$$

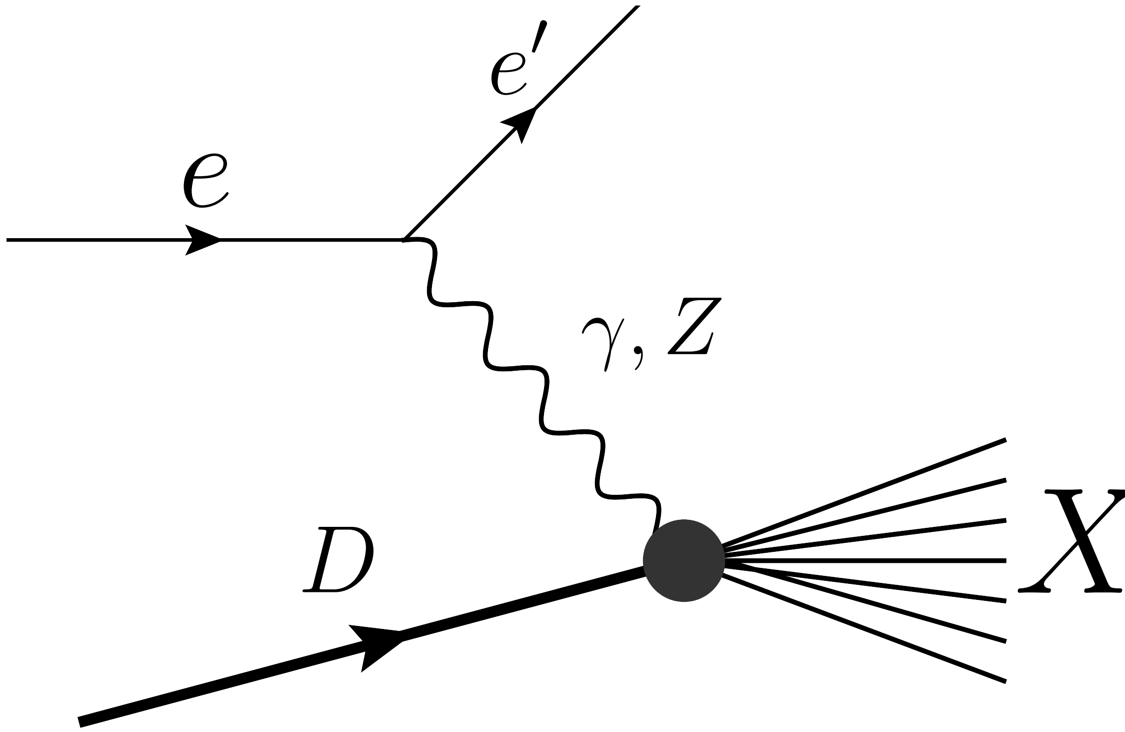

Parity-Violating Electron-Deuteron Asymmetry

$$A_{PV} = \frac{\sigma_R - \sigma_L}{\sigma_R + \sigma_L}$$

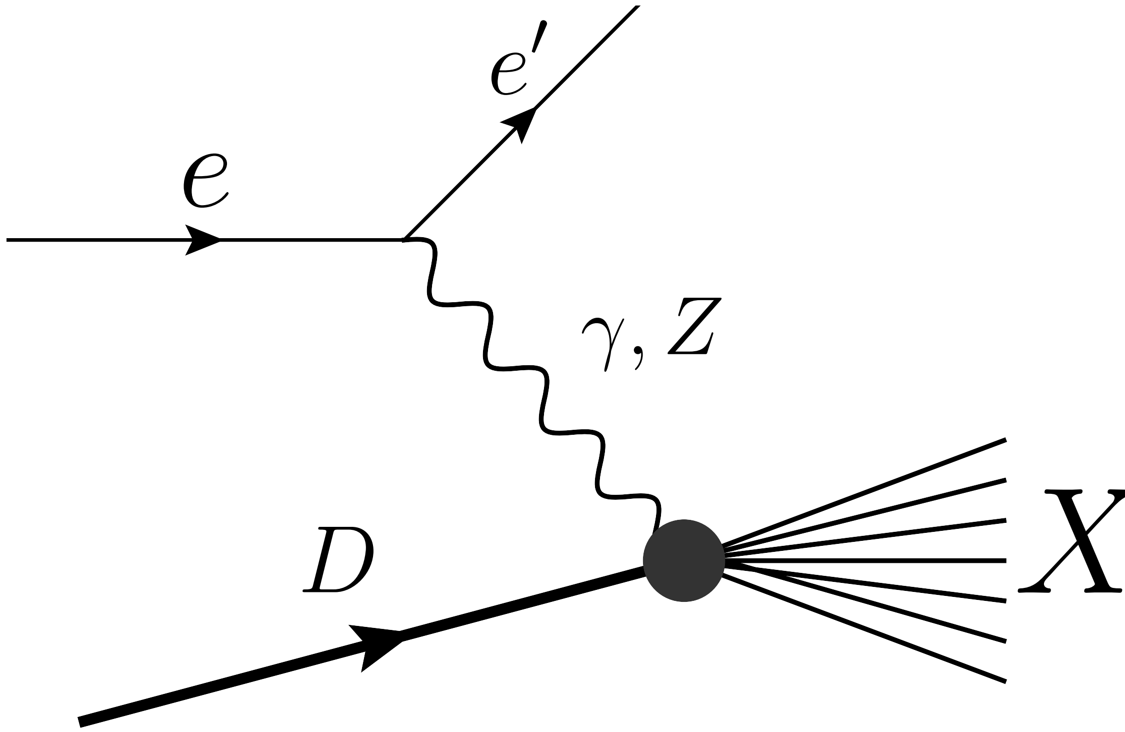

- Asymmetry in the Cahn-Gilman limit:

$$A^{RL}_{\mathrm{CG}} = -\frac{G_F Q^2}{2\sqrt{2}\pi\alpha}\frac{9}{10}\left[\left(1 - \frac{20}{9}\sin^2\theta_W\right) + \left(1 - 4\sin^2\theta_W\right)\frac{1-(1-y)^2}{1+(1-y)^2}\right]$$

Parity-Violating Electron-Deuteron Asymmetry

$$A_{PV} = \frac{\sigma_R - \sigma_L}{\sigma_R + \sigma_L}$$

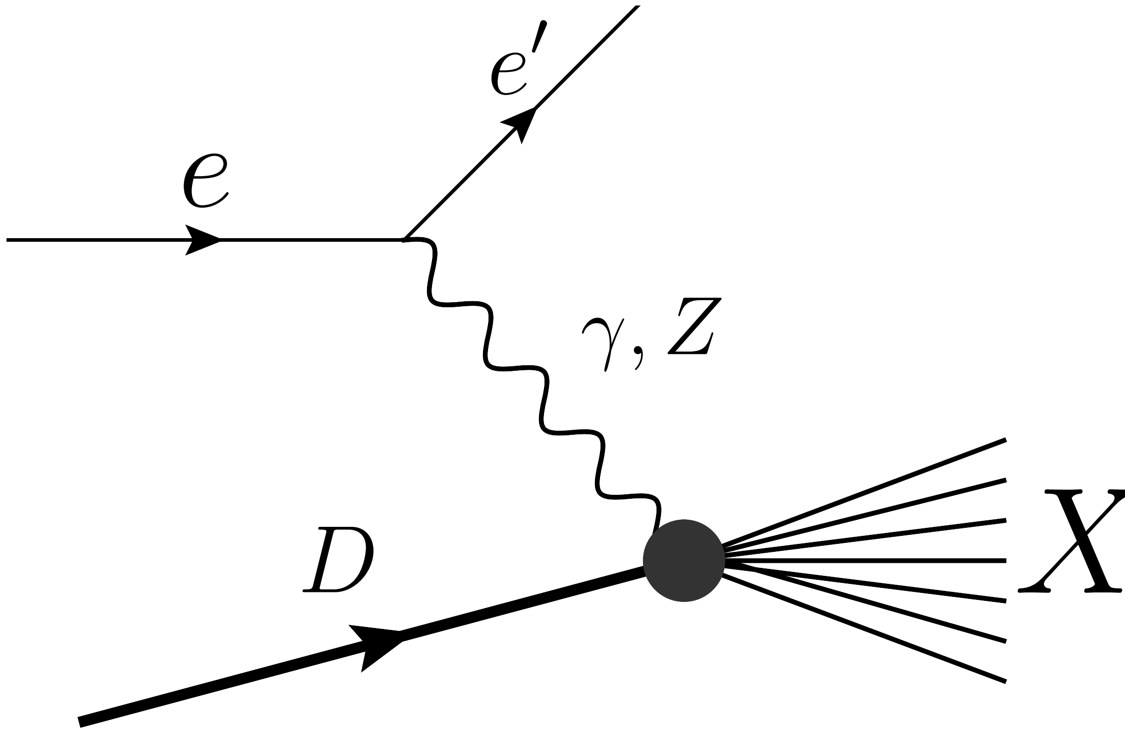

- Asymmetry in the Cahn-Gilman limit:

$$A_{\rm CG}^{RL} = -\frac{G_F Q^2}{2\sqrt{2}\pi\alpha}\frac{9}{10}\left[\left(1 - \frac{20}{9}\sin^2\theta_W\right) + \left(1 - 4\sin^2\theta_W\right)\frac{1-(1-y)^2}{1+(1-y)^2}\right]$$

Hadronic effects cancel!

[Prescott, et. al (1978)]

- Asymmetry measurement is is effectively a measurement of the weak mixing angle!

Corrections to the Cahn-Gilman Limit

- Hadronic effects appear as corrections to the Cahn-Gilman formula:

$$A_{RL} = -\frac{G_F Q^2}{2\sqrt{2}\pi\alpha}\frac{9}{10}\left[\tilde{a}_1 + \tilde{a}_2 \frac{1-(1-y)^2}{1+(1-y)^2}\right]$$

$$\tilde{a}_j = -\frac{2}{3}(2C_{ju} - C_{jd})\left[1 + R_j(\text{new}) + R_j(\text{sea}) + R_j(\text{CSV}) + R_j(\text{TMC}) + R_j(\text{HT})\right]$$

- Weak Mixing Angle
- New physics
- Sea quarks
- Charge symmetry violation
- Target mass
- Higher twist

- Hadronic effects must be well understood before any claim for evidence of new physics can be made.

[Bjorken,Hobbs,Melnitchouk;
SM, Ramsey-Musolf, Sacco;
Belitsky, Mashanov, Schafer;
Seng,Ramsey-Musolf, ….]

Contact Interactions

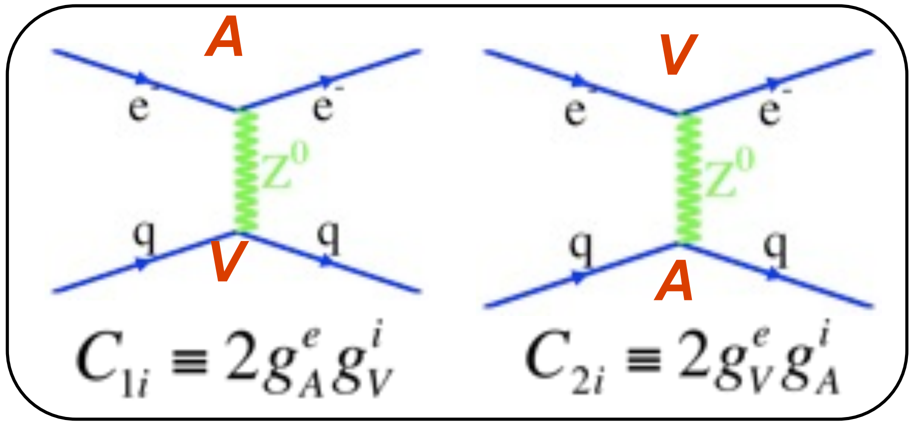

- For $Q^2 << (M_Z)^2$ limit, electron-quark scattering via the weak neutral current is mediated by contact interactions:

$$\mathcal{L} = \frac{G_F}{\sqrt{2}} \sum_q \left[C_{1q}\ \bar{\ell}\gamma^\mu\gamma_5\ell\bar{q}\gamma_\mu q + C_{2q}\ \bar{\ell}\gamma^\mu\ell\bar{q}\gamma_\mu\gamma_5 q + C_{3q}\ \bar{\ell}\gamma^\mu\gamma_5\ell\bar{q}\gamma_\mu\gamma_5 q \right]$$

- Tree-level Standard Model values:

$$C_{1u} = -\frac{1}{2} + \frac{4}{3}\sin^2(\theta_W)\ ,\quad C_{2u} = -\frac{1}{2} + 2\sin^2(\theta_W)\ ,\quad C_{3u} = \frac{1}{2}\ ,$$
$$C_{1d} = \frac{1}{2} - \frac{2}{3}\sin^2(\theta_W)\ ,\quad C_{2d} = \frac{1}{2} - 2\sin^2(\theta_W)\ ,\quad C_{3d} = -\frac{1}{2}$$

New Physics Effects

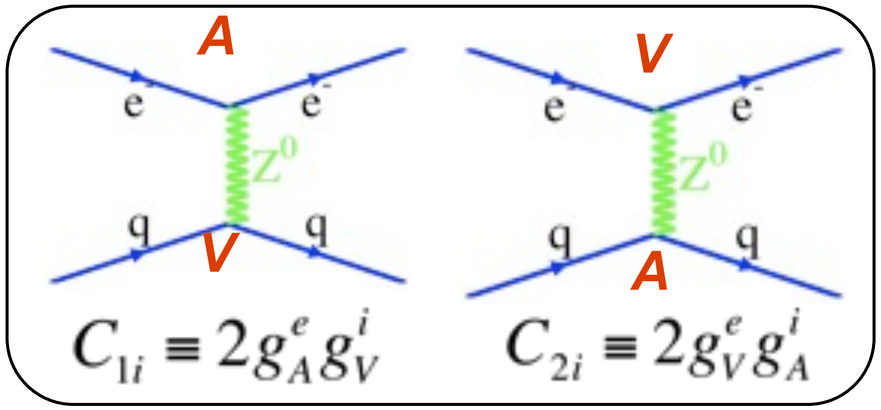

+

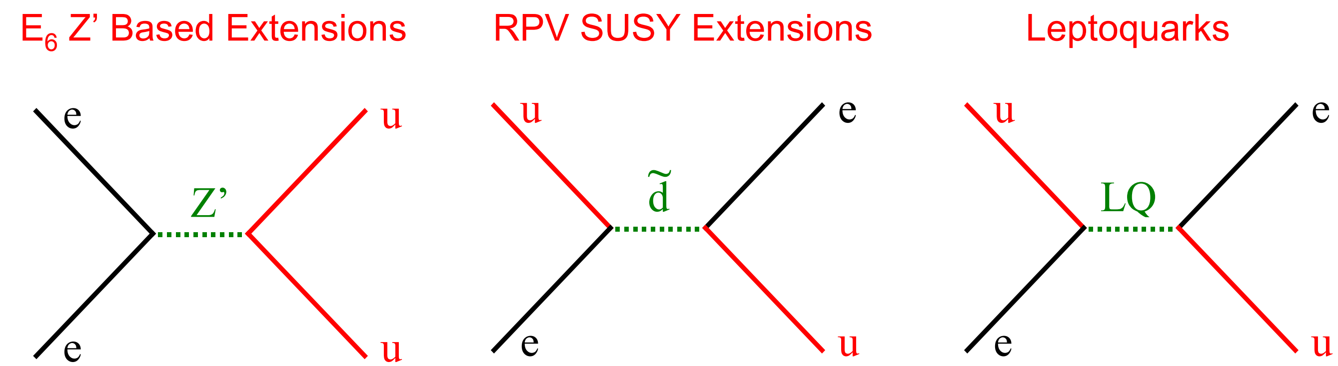

- In the $Q^2 \ll M_Z^2$ limit, electron-quark interactions via the weak neutral current can be parameterized by contact interactions:

$$\mathcal{L} = \frac{G_F}{\sqrt{2}} \sum_q \left[C_{1q}\, \bar{\ell}\gamma^\mu\gamma_5\ell\bar{q}\gamma_\mu q + C_{2q}\, \bar{\ell}\gamma^\mu\ell\bar{q}\gamma_\mu\gamma_5 q + C_{3q}\, \bar{\ell}\gamma^\mu\gamma_5\ell\bar{q}\gamma_\mu\gamma_5 q \right]$$

- New physics contact interactions arise as a shift in the WNC couplings compared to the SM prediction:

$$C_{iq} = C_{iq}(\mathrm{SM}) + \Delta C_{iq}$$

SM contribution

New Physics contribution

- Deviations from the SM prediction of the WNC couplings will lead to corresponding deviations in the extracted value of the weak mixing angle.

Accessing C_{iq} via Parity-Violating Observables

- Atomic Parity Violation (APV):
  Sensitive to C_{1q} couplings via $Q_W(Z,N)$

- Parity Violating Elastic Scattering (Qweak, P2):
  Sensitive to C_{1q} couplings through $Q_W(Z=1,N=0)$

$$Q_W(Z,N) = -2[C_{1u}(2Z+N) + C_{1d}(Z+2N)]$$

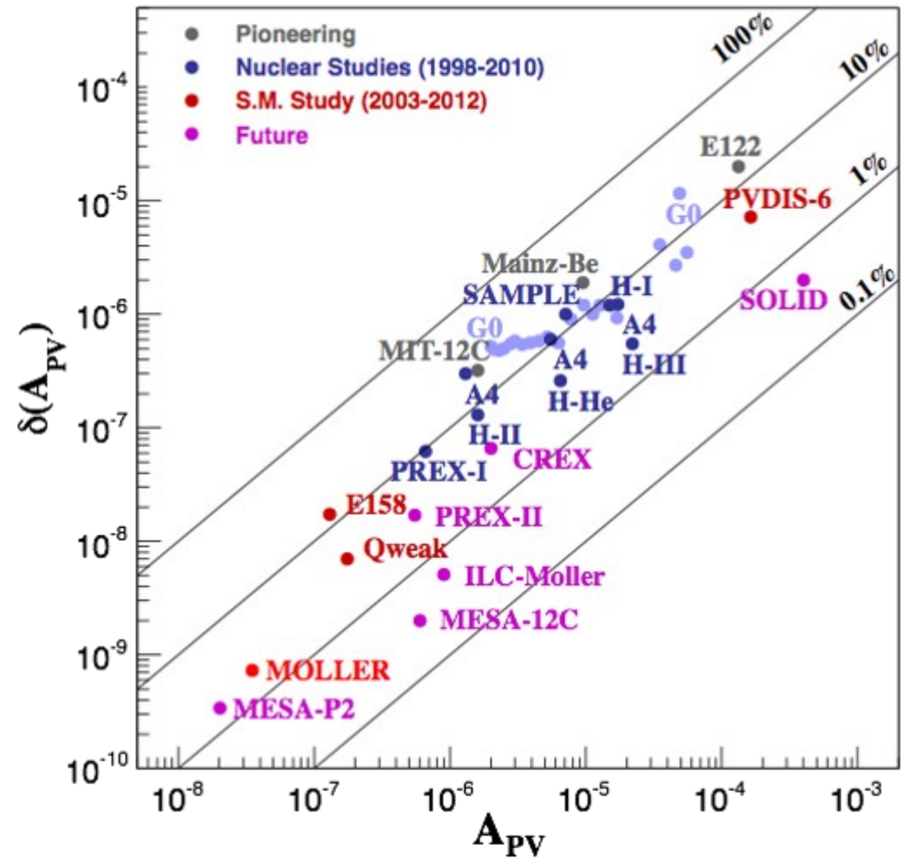

- Parity Violating DIS (E122, PVDIS-6, SOLID, EIC):
  Sensitive to C_{1q} and C_{2q}

$$A_{PV}^{DIS} = \frac{G_F Q^2}{4\sqrt{2}(1+Q^2/M_Z^2)\pi\alpha}\left[a_1 + \frac{1-(1-y)^2}{1+(1-y)^2}a_3\right]$$

$$a_1 = \frac{2\sum_q e_q C_{1q}(q+\bar{q})}{\sum_q e_q^2(q+\bar{q})} \qquad a_3 = \frac{2\sum_q e_q C_{2q}(q-\bar{q})}{\sum_q e_q^2(q+\bar{q})}$$

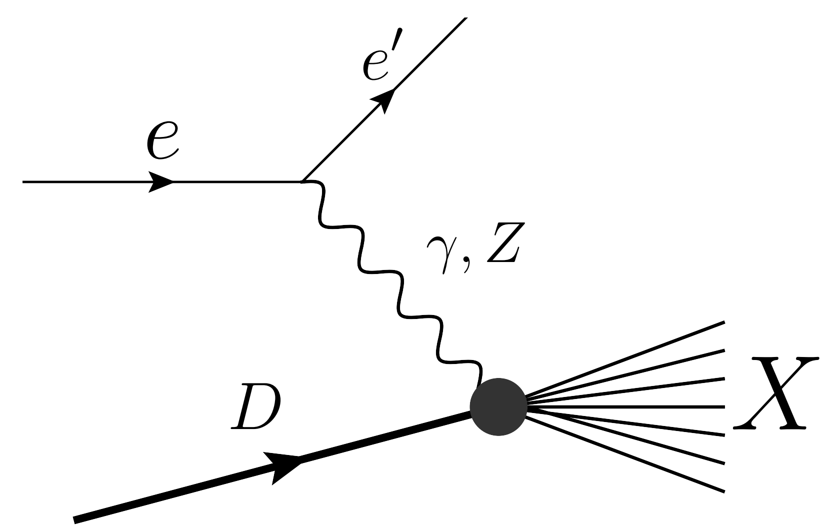

For the isocalar deuteron target, structure function effects largely cancel

Status of WNC Couplings

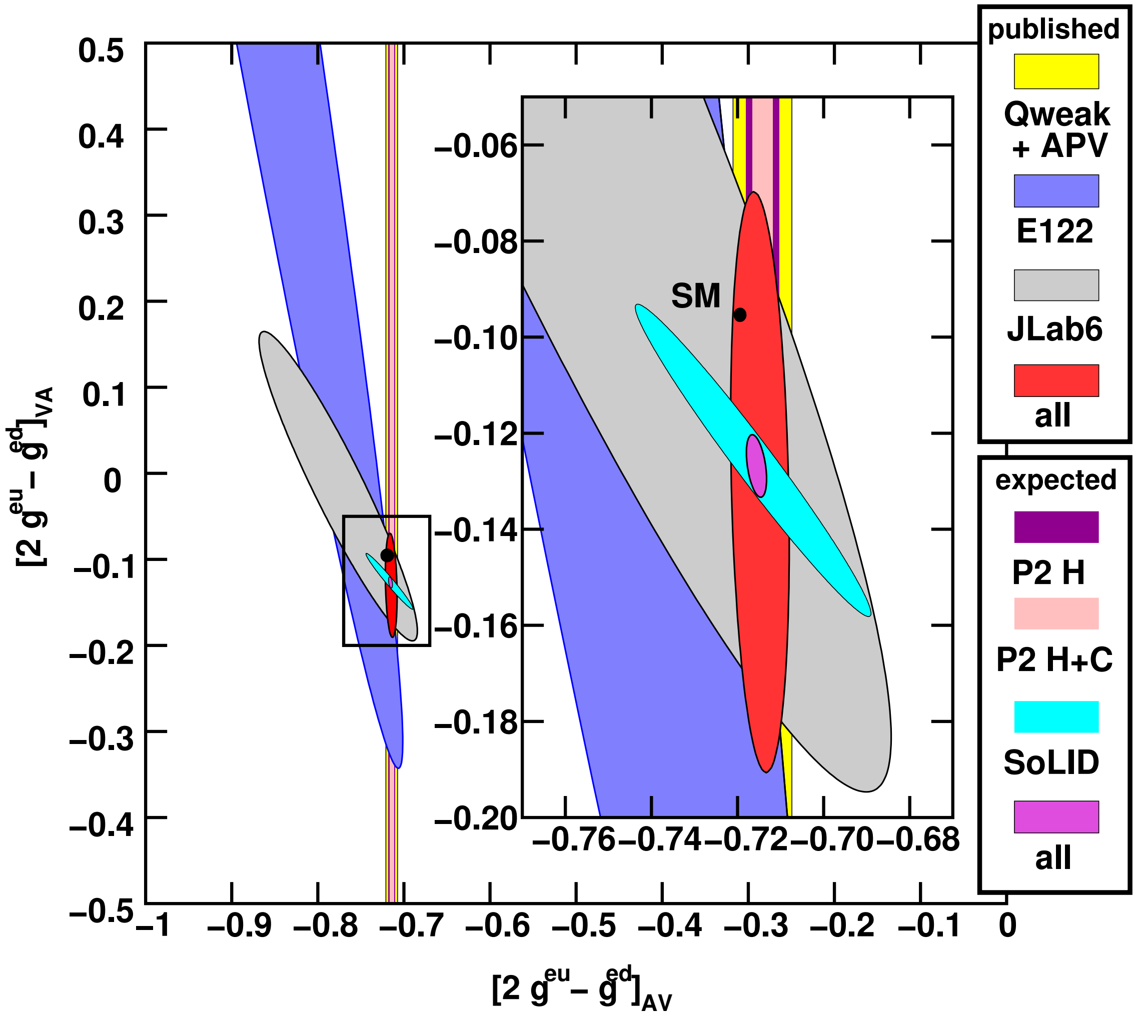

arXiv:2209.13357, SoLID White Paper

FIG. 13. Adapted from Ref. [63]: Current experimental knowledge of the couplings g^{eq}_{VA} (vertical axis). The latest world data constraint (red ellipse) is provided by combining the 6 GeV Qweak [51] on g^{eq}_{AV} (yellow vertical band) and the JLab 6 GeV PVDIS [53, 54] experiments (grey ellipse). The SoLID projected result is shown as the cyan ellipse. Also shown are expected results from P2 (purple and pink vertical bands) and the combined projection using SoLID, P2, and all existing world data (magenta ellipse), centered at the current best fit values.

- The combination $2C_{1u} - C_{1d}$ is severely constrained by Qweak and Atomic Parity violation.
- The combination $2C_{2u} - C_{2d}$ is known to within ~50% from the JLAB 6 GeV experiment:

$$2C_{2u} - C_{2d} = -0.145 \pm 0.068$$

- SOLID is expected significantly improve on this result.

Leptophobic Z'

- Leptophobic Z's are an interesting BSM scenario since they only shifts the C_{2q} couplings in A_{PV}

- Leptophobic Z's only affect the b(x) term or the C_{2q} coefficients in A_{PV}:

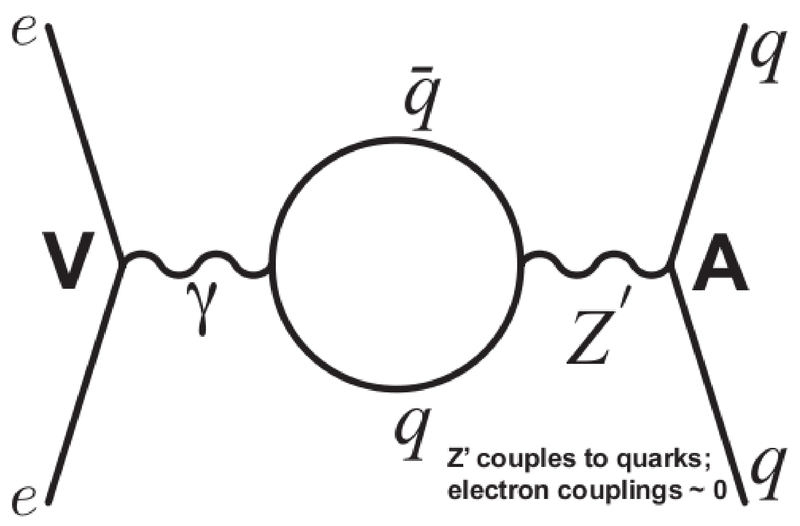

Leptophobic Z' contributes only to the C_{2q} couplings!

[M.Alonso-Gonzalez, M.Ramsey-Musolf;
M.Buckley,M.Ramsey-Musolf]

$$A_{\mathrm{PV}}^{\mathrm{DIS}} = \frac{G_F Q^2}{4\sqrt{2}(1+Q^2/M_Z^2)\pi\alpha}\left[a_1 + \frac{1-(1-y)^2}{1+(1-y)^2} a_3\right]$$

Probing the Dark Sector

- Strong evidence for dark matter through gravitational effects:
  - Galactic Rotation Curves
  - Gravitational Lensing
  - Cosmic Microwave Background
  - Large Scale Structure Surveys

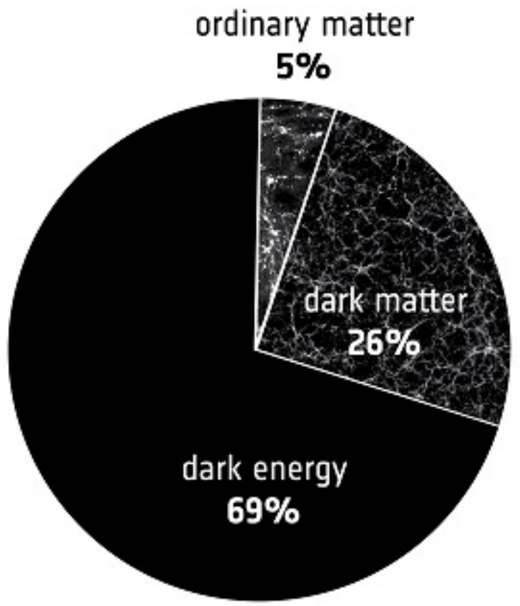

- WIMP dark matter paradigm
  - Mass ~ TeV
  - Weak interaction strength couplings
  - Gives the required relic abundance

- However, so far no direct evidence for WIMP dark matter

- Perhaps dark sector has a rich structure including different species and gauge forces, just like the visible sector

Dark Photon Scenario

[Also see talks by Neil, Liu]

- Dark $U(1)_d$ gauge group
- Interacts with SM via kinetic mixing (and mass mixing)

$$\mathcal{L} \supset -\frac{1}{4}F'_{\mu\nu}F'^{\mu\nu} + \frac{m_{A'}^2}{2}A'_\mu A'^\mu + \frac{\epsilon}{2\cos\theta_W}F'_{\mu\nu}B^{\mu\nu}$$

- The mixing induces a coupling of the dark photon to the electromagnetic and weak neutral currents.

$$\mathscr{L}_{int} = -e\epsilon J^\mu_{em} A'_\mu$$

- Could help explain astrophysical data and anomalies

[Arkani-Hamed, Finkbeiner, Slatyer, Wiener, ...]

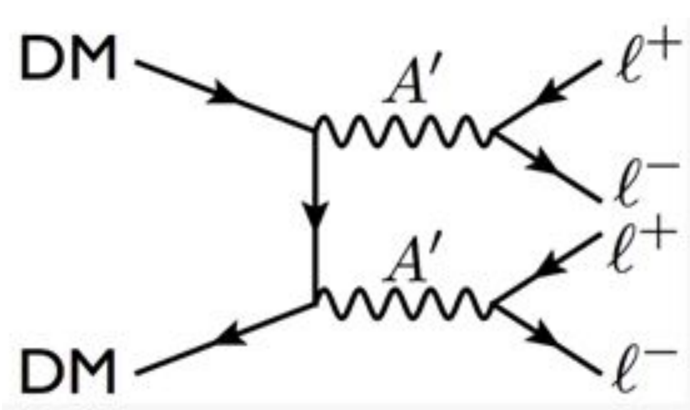

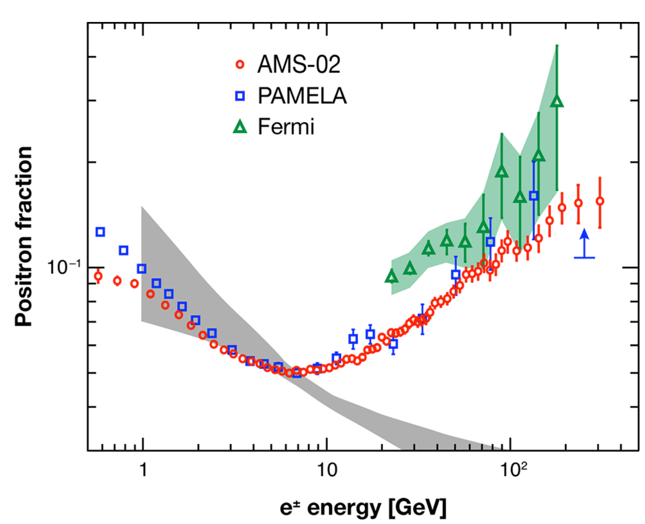

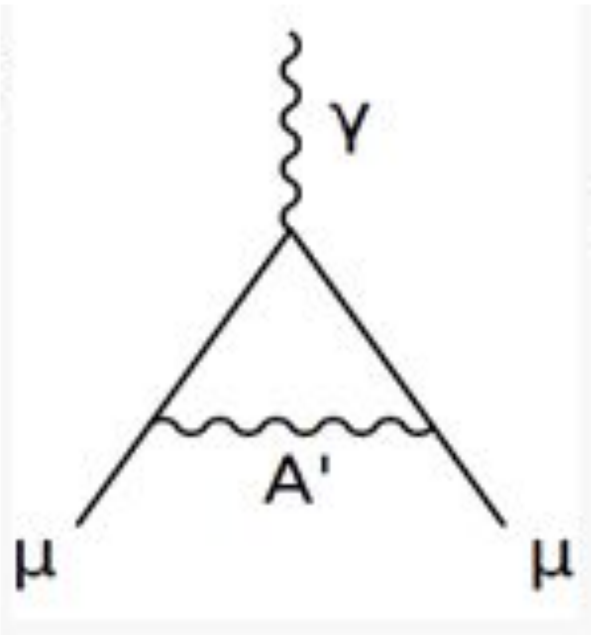

Dark Photon Scenario

- Active experimental program to search for dark photons
[Bjorken, Essig, Schuster, Toro; Baten, Pospelov, Ritz; Izaguirre Krnjaic, Schuster, Toro]

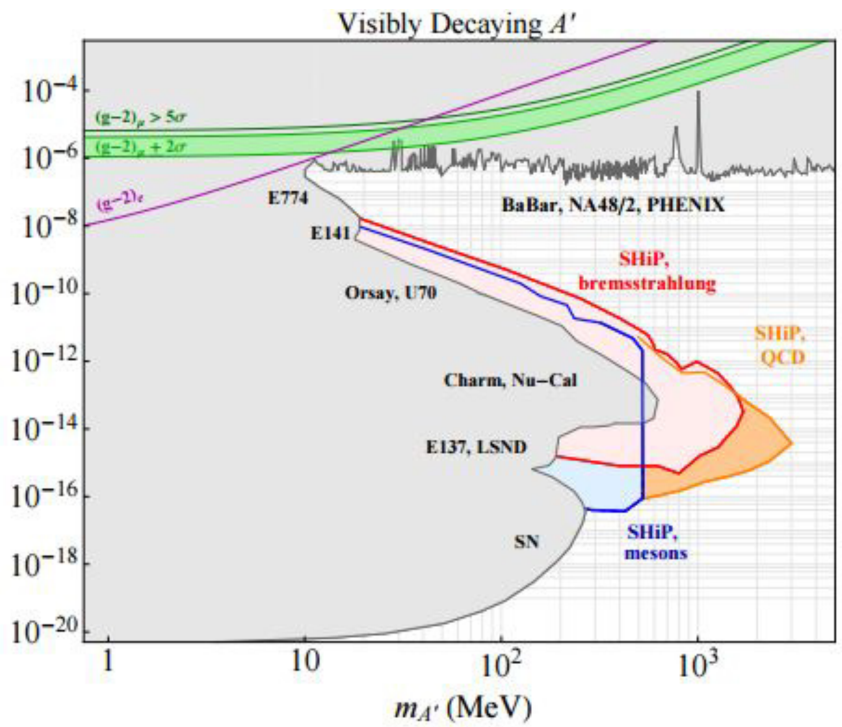

S. Alekhin *et al.*, arXiv:1504.04855 [hep-ph]

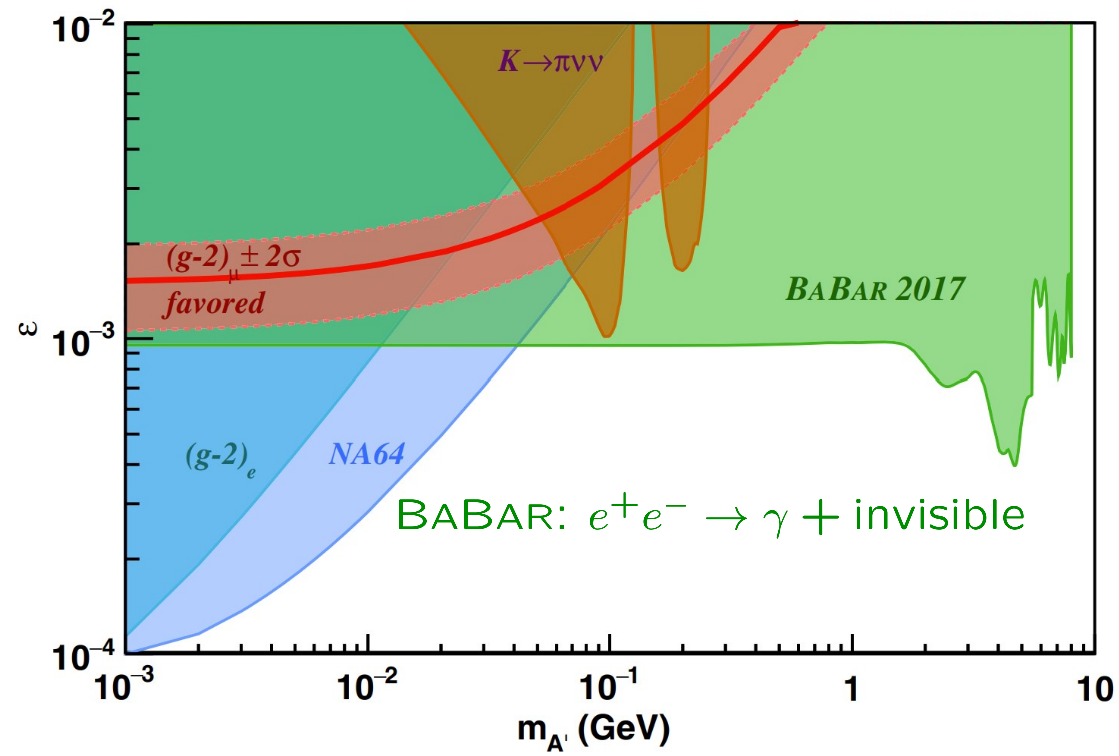

- Beam Dump Experiments:

[Bjorken, Essig, Schuster, Toro]

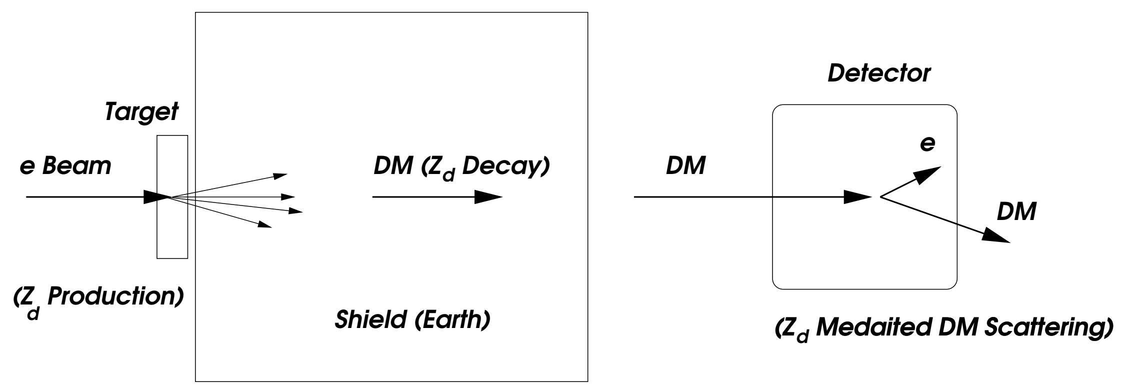

Dark Photon Scenario: Impact on PVES

[Thomas, Wang, Williams]

$$\mathcal{L} \supset -\frac{1}{4}F'_{\mu\nu}F'^{\mu\nu} + \frac{m_{A'}^2}{2}A'_\mu A'^\mu + \frac{\epsilon}{2\cos\theta_W}F'_{\mu\nu}B^{\mu\nu}$$

- Constraints on Dark Photon parameter space will be independent of the details of the decay branching fractions of the dark photon

- For a light dark photon, the induced coupling to the weak neutral coupling is suppressed (due to a cancellation between the kinetic and mass mixing induced couplings). [Gopalakrishna, Jung, Wells; Davoudiasl, Lee, Marciano]

- Let's consider a heavier dark photon for a sizable coupling to the weak neutral current and a correspondingly sizable effect in PVES. [Thomas, Wang, Williams]

Dark Photon Scenario: Impact on PVES

[Thomas, Wang, Williams]

$$\mathcal{L} \supset -\frac{1}{4}F'_{\mu\nu}F'^{\mu\nu} + \frac{m^2_{A'}}{2}A'_\mu A'^\mu + \frac{\epsilon}{2\cos\theta_W}F'_{\mu\nu}B^{\mu\nu}$$

- The usual PVDIS asymmetry has the form:

$$A_{\rm PV}^{\rm DIS} = \frac{G_F Q^2}{4\sqrt{2}(1+Q^2/M_Z^2)\pi\alpha}\left[a_1 + \frac{1-(1-y)^2}{1+(1-y)^2}a_3\right]$$

- Including the effects of a dark photon, we get additional terms:

$$A_{\rm PV} = \frac{Q^2}{2\sin^2 2\theta_W(Q^2+M_Z^2)}\left[a_1^{\gamma Z} + \frac{1-(1-y)^2}{1+(1-y)^2}a_3^{\gamma Z} + \frac{Q^2+M_Z^2}{Q^2+M_{A_D}^2}\left(a_1^{\gamma A_D} + \frac{1-(1-y)^2}{1+(1-y)^2}a_3^{\gamma A_D}\right)\right],$$

Dark Photon Scenario: Impact on PVES

- Equivalent to working with the usual PVDIS formula:

$$A_{\rm PV}^{\rm DIS} = \frac{G_F Q^2}{4\sqrt{2}(1+Q^2/M_Z^2)\pi\alpha}\left[a_1 + \frac{1-(1-y)^2}{1+(1-y)^2}a_3\right]$$

- But with shifted C_{iq} couplings:

$$C_{1q} = C_{1q}^Z + \frac{Q^2+M_Z^2}{Q^2+M_{A_D}^2}C_{1q}^{A_D} = C_{1q}^{\rm SM}(1+R_{1q})$$

$$C_{2q} = C_{2q}^Z + \frac{Q^2+M_Z^2}{Q^2+M_{A_D}^2}C_{2q}^{A_D} = C_{2q}^{\rm SM}(1+R_{2q})$$

[Thomas, Wang, Williams]

Dark Photon Scenario: Shift in C_{iq} (PVDIS, HERA)

[Thomas, Wang, Williams]

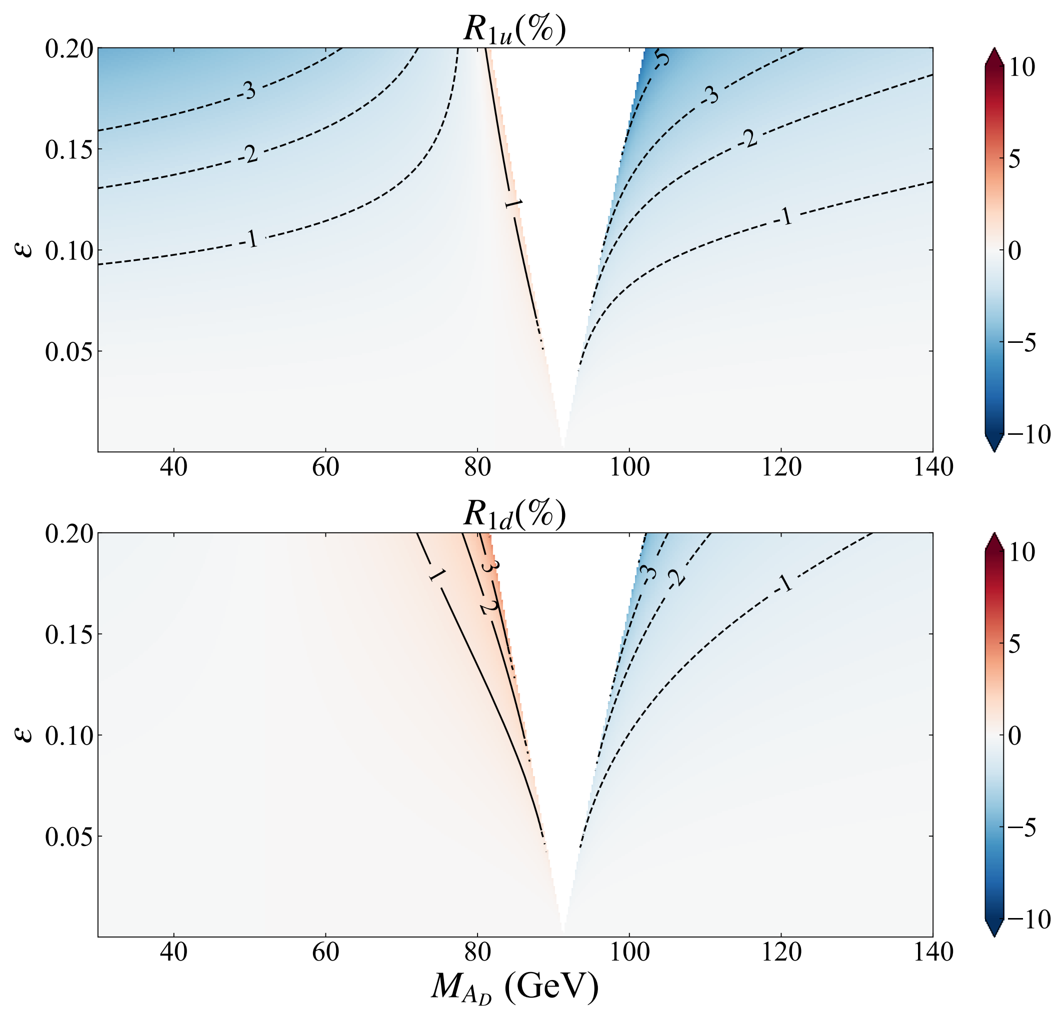

FIG. 2. The correction factors R_{1u} and R_{1d} at $Q^2 = M_Z^2$.

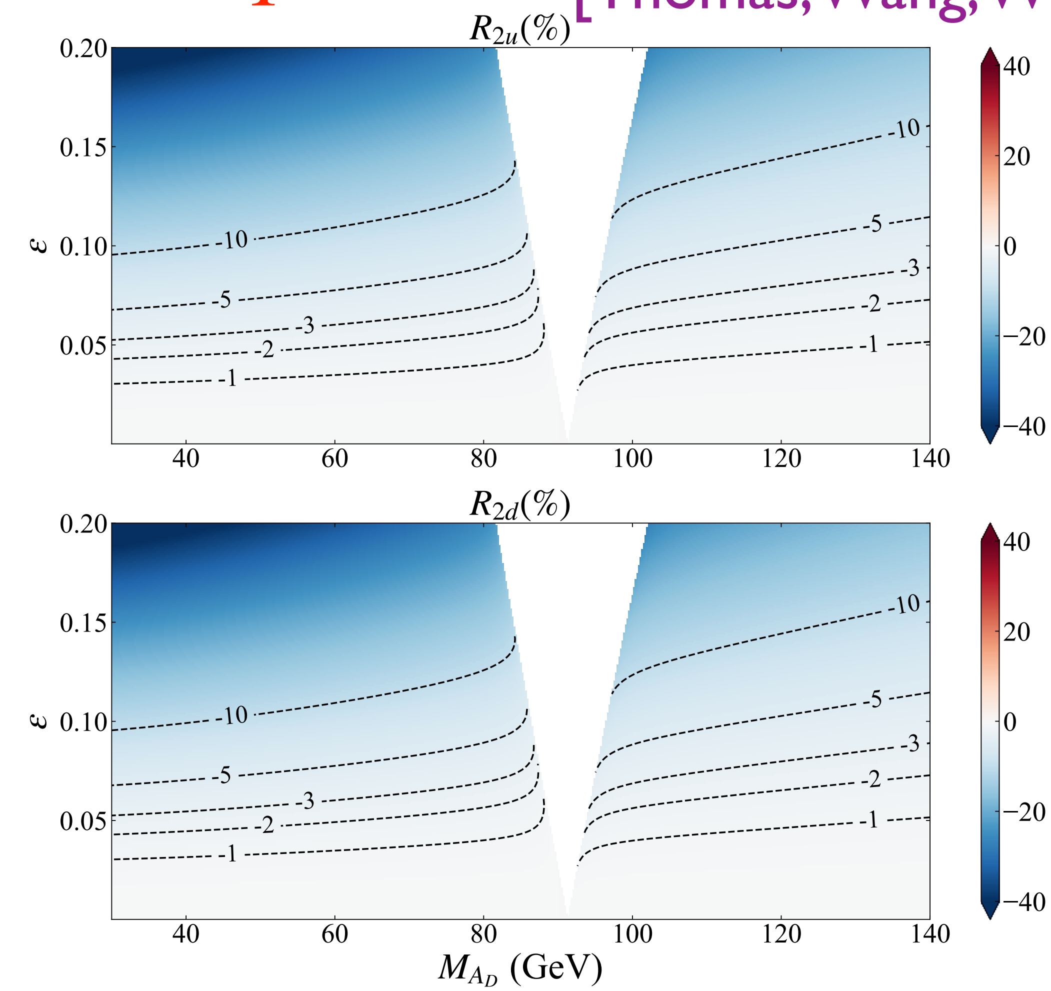

FIG. 3. The correction factors R_{2u} and R_{2d} at $Q^2 = M_Z^2$.

$$C_{1q} = C_{1q}^Z + \frac{Q^2 + M_Z^2}{Q^2 + M_{A_D}^2} C_{1q}^{A_D} = C_{1q}^{\mathrm{SM}}(1 + R_{1q})$$

$$C_{2q} = C_{2q}^Z + \frac{Q^2 + M_Z^2}{Q^2 + M_{A_D}^2} C_{2q}^{A_D} = C_{2q}^{\mathrm{SM}}(1 + R_{2q})$$

- Study could be easily extended to EIC kinematics.

Light Dark-Z Parity Violation

[Davoudiasl, Lee, Marciano]

- An interesting scenario is that of a “light” Dark-Z.

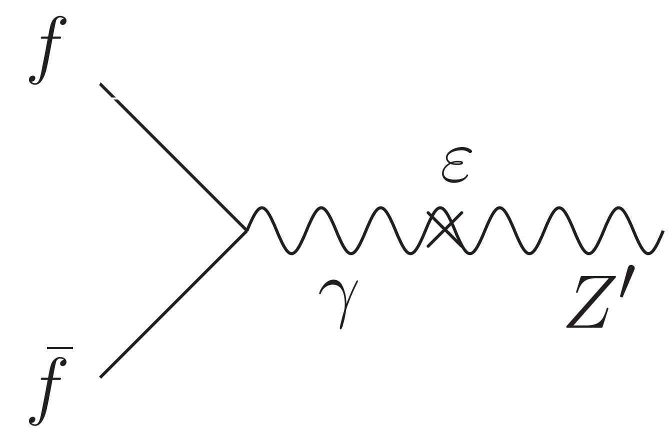

- The standard kinetic mixing scenario:

$$\mathcal{L}_{\text{gauge}} = -\frac{1}{4}B_{\mu\nu}B^{\mu\nu} + \frac{1}{2}\frac{\varepsilon}{\cos\theta_W}B_{\mu\nu}Z_d^{\mu\nu} - \frac{1}{4}Z_{d\mu\nu}Z_d^{\mu\nu}$$

- And additional mass mixing (for example, from extended Higgs sector) can induce sizable dark-Z coupling to the weak neutral current:

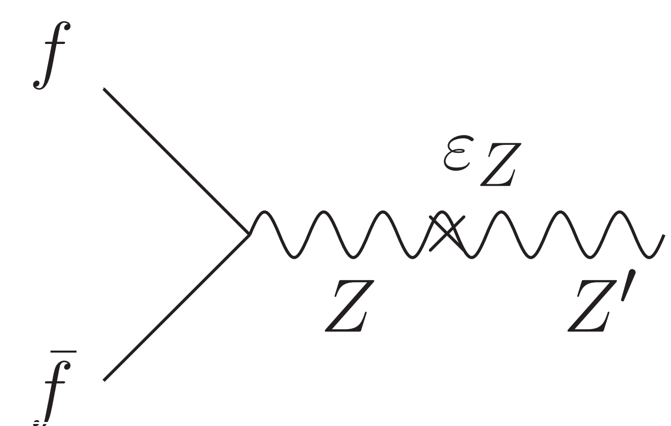

$$M_0^2 = m_Z^2 \begin{pmatrix} 1 & -\varepsilon_Z \\ -\varepsilon_Z & m_{Z_d}^2/m_Z^2 \end{pmatrix}$$

$$\varepsilon_Z = \frac{m_{Z_d}}{m_Z}\delta$$

- Dark-Z couples to the electromagnetic and neutral current coupling:

$$\mathcal{L}_{\text{int}} = \left(-e\varepsilon J_\mu^{em} - \frac{g}{2\cos\theta_W}\varepsilon_Z J_\mu^{NC}\right) Z_d^\mu$$

Light Dark-Z Parity Violation

[Davoudiasl, Lee, Marciano]

- Effective change in presence of dark-Z for parity violating asymmetries:

$$G_F \to \rho_d G_F$$

$$\sin^2\theta_W \to \kappa_d \sin^2\theta_W$$

$$\rho_d = 1 + \delta^2 \frac{m_{Z_d}^2}{Q^2 + m_{Z_d}^2}$$

$$\kappa_d = 1 - \frac{\varepsilon}{\varepsilon_Z}\delta^2 \frac{\cos\theta_W}{\sin\theta_W} \frac{m_{Z_d}^2}{Q^2 + m_{Z_d}^2}$$

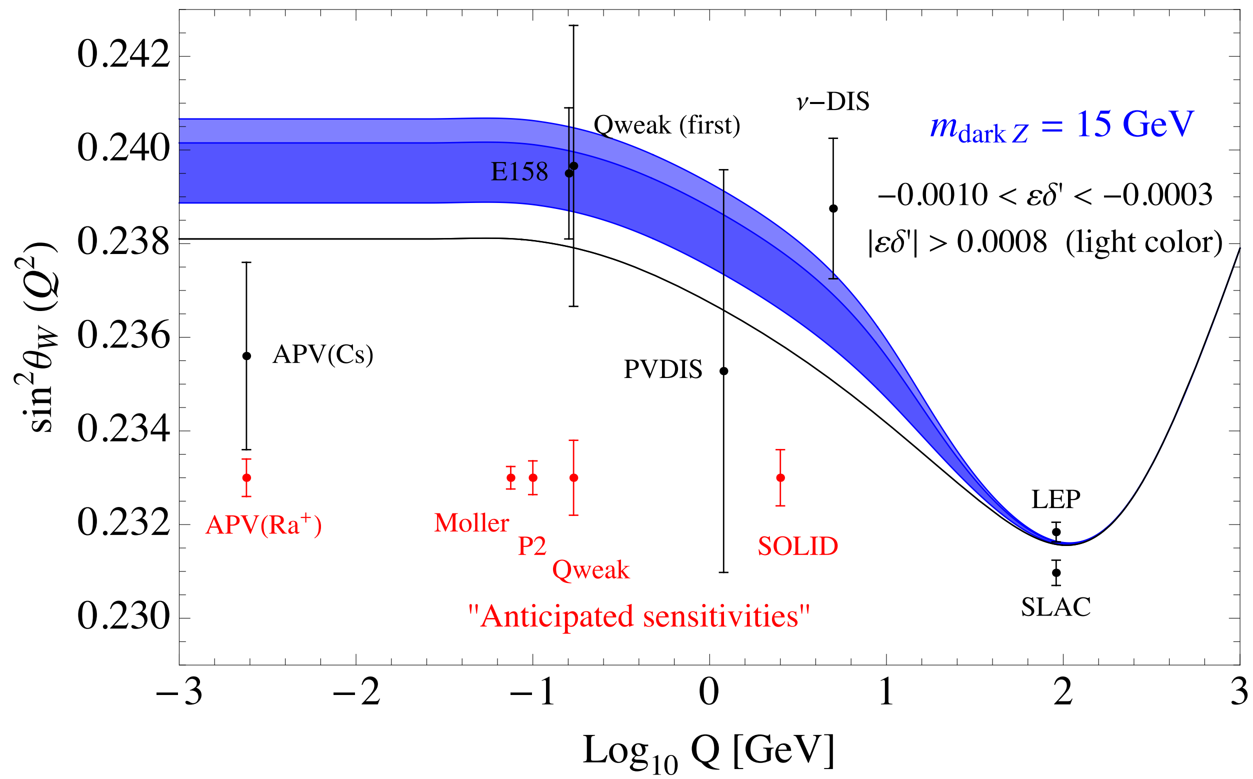

- Constraints from Higgs Decay:

$$H \to Z Z_d \to \ell_1^+ \ell_1^- \ell_2^+ \ell_2^-$$

$$|\varepsilon\delta'| \lesssim 0.0008$$

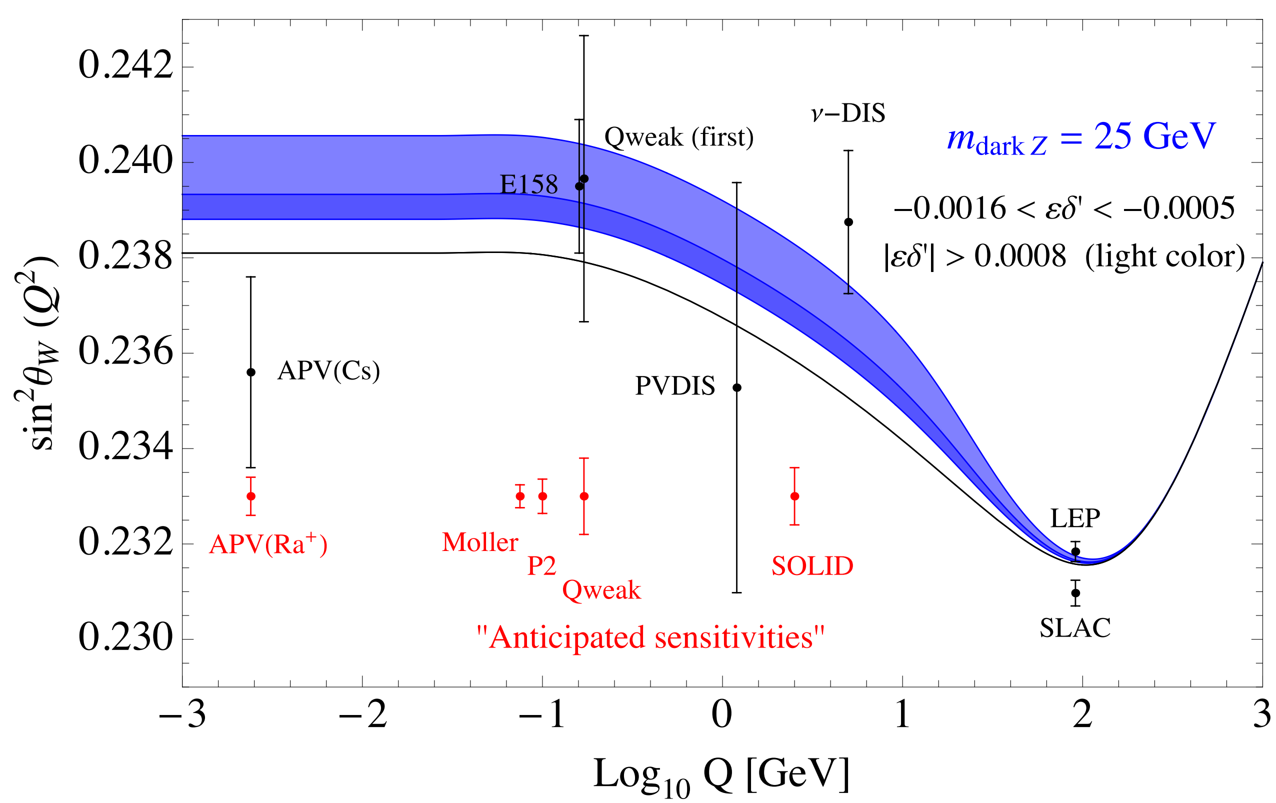

- Note that this constraint will be much weaker if the Dark Z has a larger branching fraction to the dark sector.

EIC/ECCE Simulation Studies

[Boughezal, Emmert, Kutz, SM, Nycz,Petriello, Simsek,Wiegand, Zheng]

- Energy and integrated luminosity configurations used in the study:

Electron-Deuteron PVDIS		Electron-Proton PVDIS	
D1	5 GeV $\times$ 41 GeV eD, 4.4 fb^{-1}	P1	5 GeV $\times$ 41 GeV ep, 4.4 fb^{-1}
D2	5 GeV $\times$ 100 GeV eD, 36.8 fb^{-1}	P2	5 GeV $\times$ 100 GeV ep, 36.8 fb^{-1}
D3	10 GeV $\times$ 100 GeV eD, 44.8 fb^{-1}	P3	10 GeV $\times$ 100 GeV ep, 44.8 fb^{-1}
D4	10 GeV $\times$ 137 GeV eD, 100 fb^{-1}	P4	10 GeV $\times$ 275 GeV ep, 100 fb^{-1}
D5	18 GeV $\times$ 137 GeV eD, 15.4 fb^{-1}	P5	18 GeV $\times$ 275 GeV ep, 15.4 fb^{-1}
		P6	18 GeV $\times$ 275 GeV ep, 100 fb^{-1}

- Also considered High Luminosity (HL) configurations corresponding to an increase by a factor of 10.

- 20 million MC events generated DJANGOH + fast smearing method for each of the configurations above. 10 million events for all Q^2 and 10 million for $Q^2 > 50\ \text{GeV}^2$.

- Also, considered possibility of a positron beam.

- Observables studied:

$$A_{PV}^{e},\quad A_{PV}^{p},\quad A_{PV}^{D},\quad A_{LC}^{p},\quad A_{LC}^{D}$$

Electron-Deuteron PVDIS Asymmetry(A^{e}_{PV})

Cahn-Gilman Limit — Include strange quarks

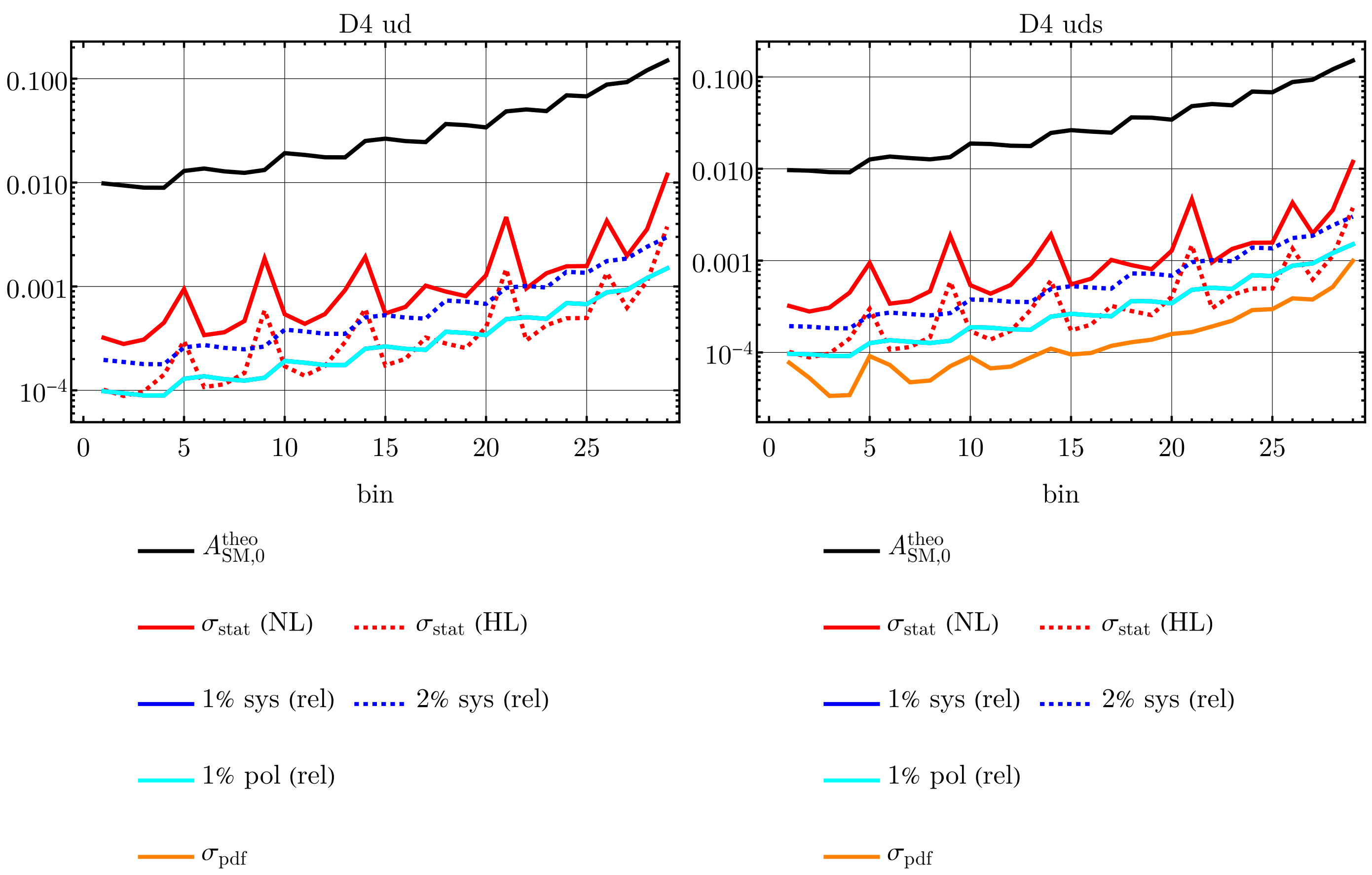

FIG. 6. Comparison of the uncertainty components for the data set D4 in the valence-only scenario (ud) and with the contributions from the sea quarks (uds). Here, "NL" refers to the currently planned annual luminosity of the EIC, while "HL" refers to a potential ten-fold luminosity upgrade.

- Statistical uncertainty dominates
- PDF uncertainty has a small impact

[Boughezal, Emmert, Kutz, SM, Nycz, Petriello, Simsek, Wiegand, Zheng]

D1	5 GeV × 41 GeV eD, 4.4 fb^{-1}	P1	5 GeV × 41 GeV ep, 4.4 fb^{-1}
D2	5 GeV × 100 GeV eD, 36.8 fb^{-1}	P2	5 GeV × 100 GeV ep, 36.8 fb^{-1}
D3	10 GeV × 100 GeV eD, 44.8 fb^{-1}	P3	10 GeV × 100 GeV ep, 44.8 fb^{-1}
D4	10 GeV × 137 GeV eD, 100 fb^{-1}	P4	10 GeV × 275 GeV ep, 100 fb^{-1}
D5	18 GeV × 137 GeV eD, 15.4 fb^{-1}	P5	18 GeV × 275 GeV ep, 15.4 fb^{-1}
		P6	18 GeV × 275 GeV ep, 100 fb^{-1}

Electron-Proton PVDIS Asymmetries: A^e_{PV} and A^p_{PV}

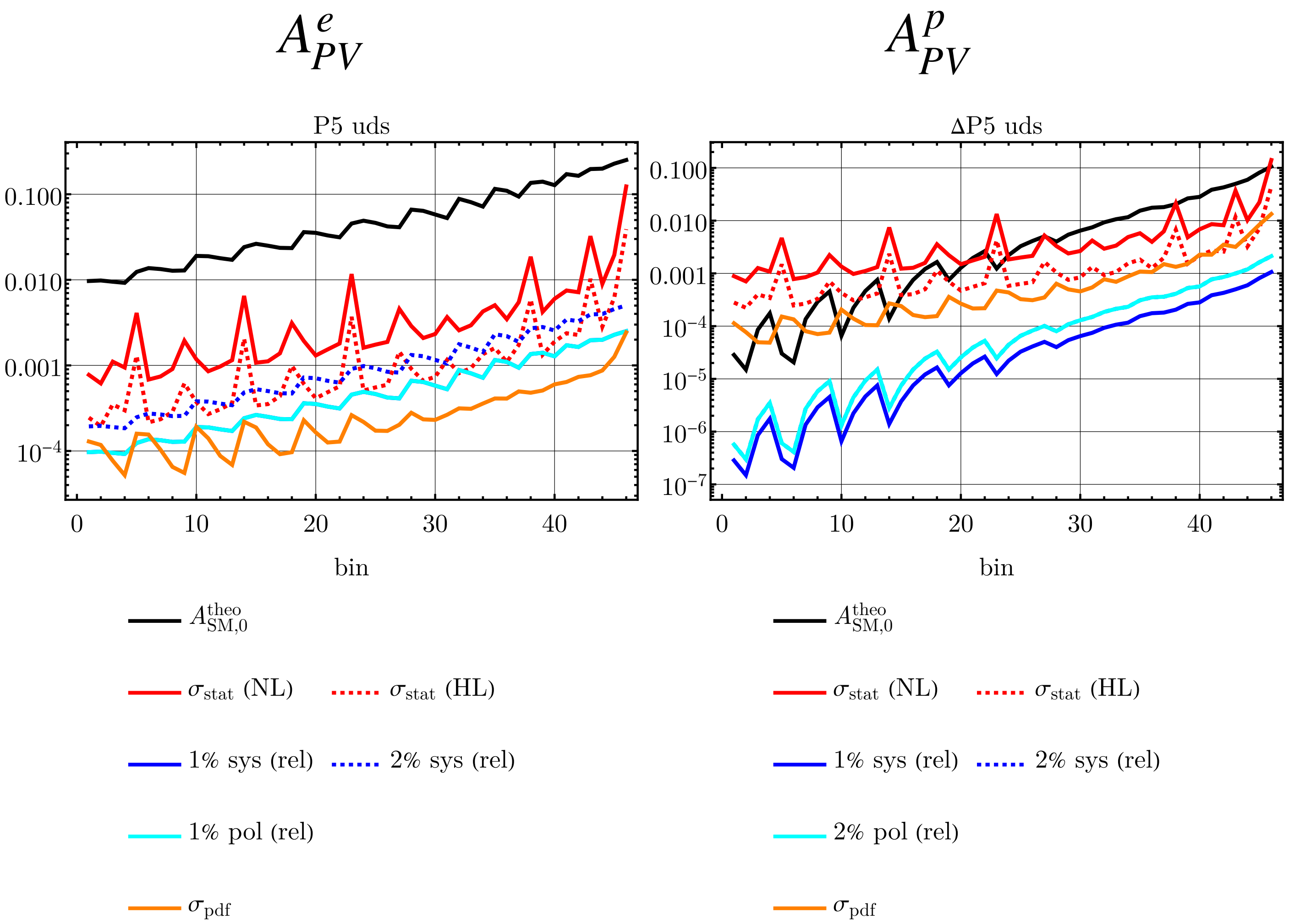

- Statistical uncertainty dominates
- PDF uncertainties have a small impact for A^e_{PV} but a significant impact for A^p_{PV}

[Boughezal, Emmert, Kutz, SM, Nycz, Petriello, Simsek, Wiegand, Zheng]

D1	5 GeV × 41 GeV eD, 4.4 fb^{-1}	P1	5 GeV × 41 GeV ep, 4.4 fb^{-1}
D2	5 GeV × 100 GeV eD, 36.8 fb^{-1}	P2	5 GeV × 100 GeV ep, 36.8 fb^{-1}
D3	10 GeV × 100 GeV eD, 44.8 fb^{-1}	P3	10 GeV × 100 GeV ep, 44.8 fb^{-1}
D4	10 GeV × 137 GeV eD, 100 fb^{-1}	P4	10 GeV × 275 GeV ep, 100 fb^{-1}
D5	18 GeV × 137 GeV eD, 15.4 fb^{-1}	P5	18 GeV × 275 GeV ep, 15.4 fb^{-1}
		P6	18 GeV × 275 GeV ep, 100 fb^{-1}

Precision Extraction of the Weak Mixing Angle

Projection for Extraction of the Weak Mixing Angle

Electron-Deuteron PVDIS (A^e_{PV})

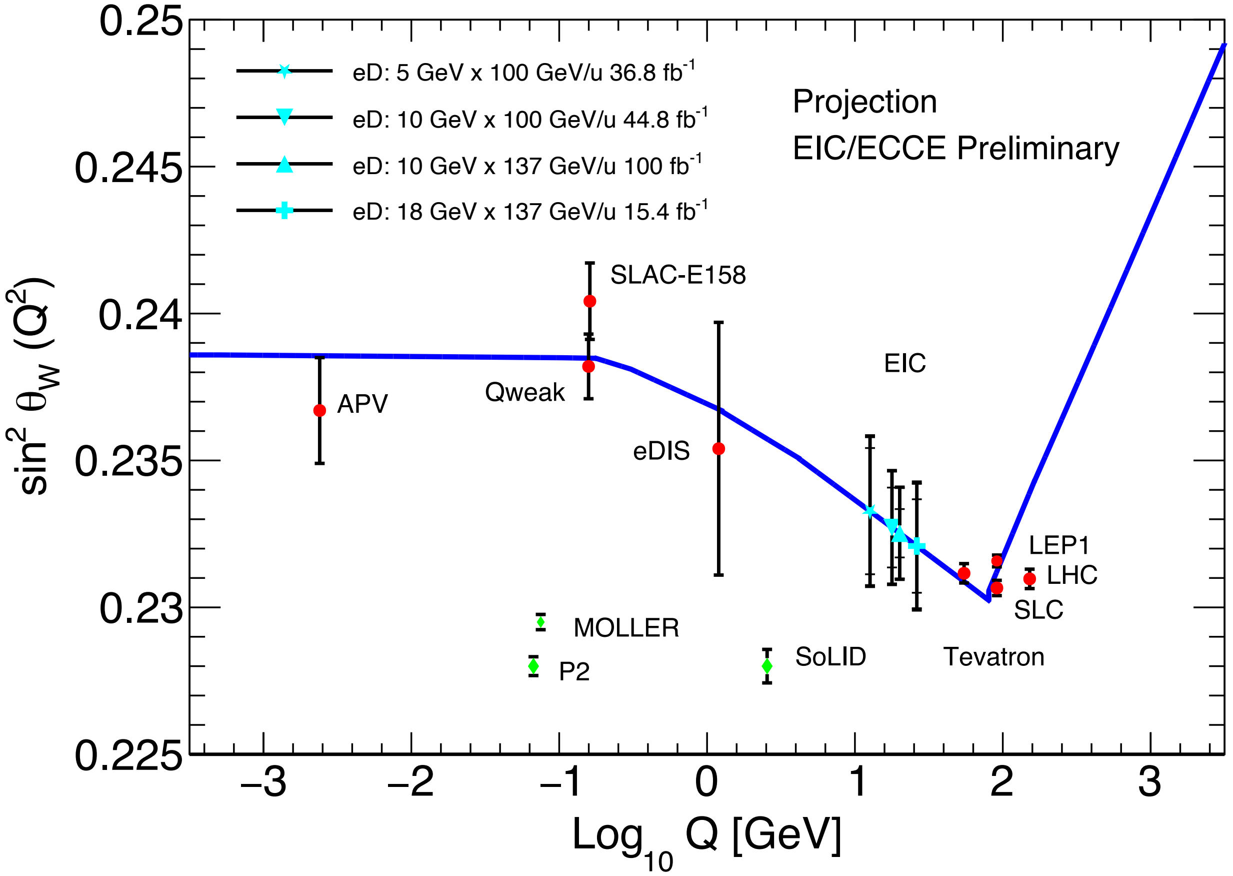

Electron-Proton PVDIS (A^e_{PV})

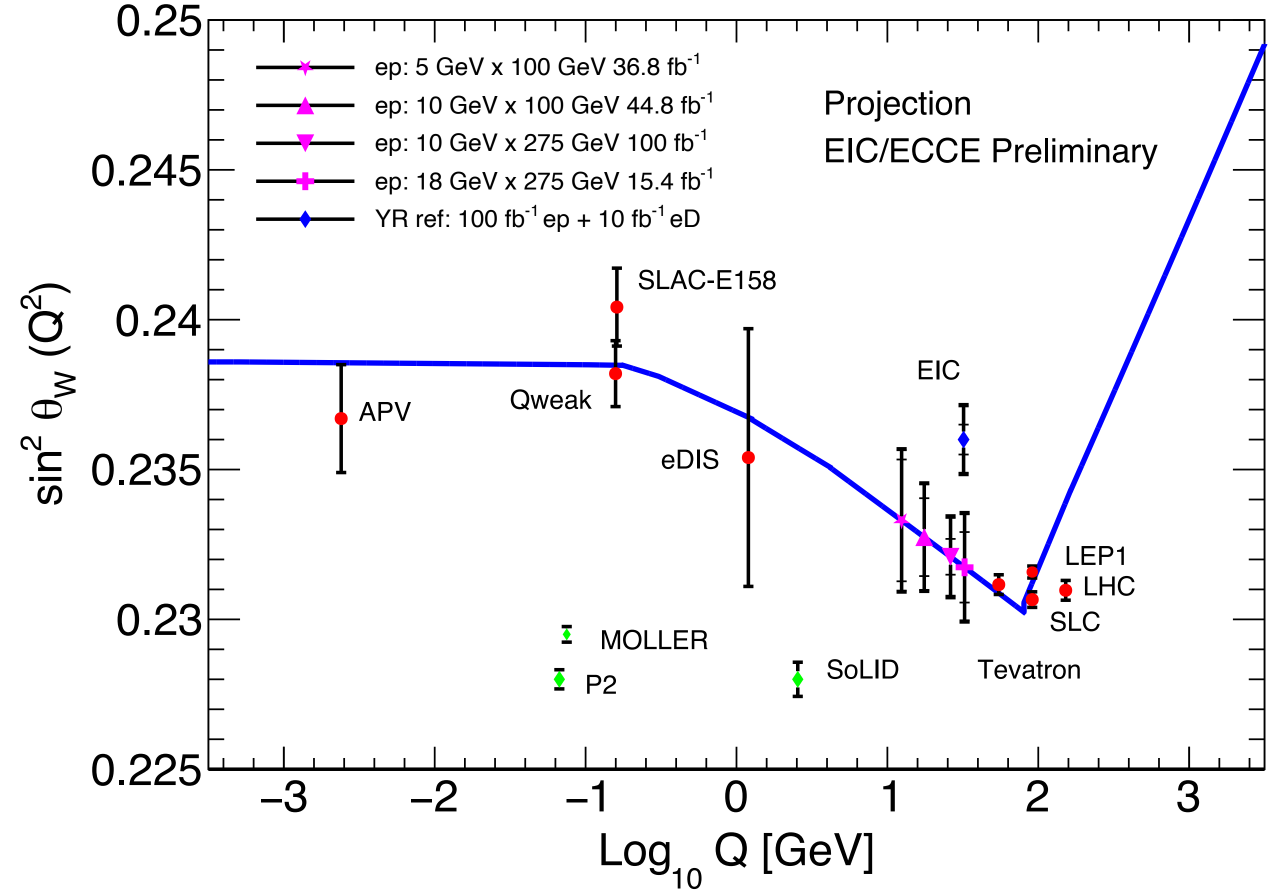

[Boughezal, Emmert, Kutz, SM, Nycz, Petriello, Simsek, Wiegand, Zheng]

- The EIC can extract the weak mixing angle over a previously unexplored range of Q^2
- Analysis included one loop $\overline{MS}$ running including particle thresholds between Q^2 and M_Z

D1	5 GeV × 41 GeV eD, 4.4 fb^{-1}	P1	5 GeV × 41 GeV ep, 4.4 fb^{-1}
D2	5 GeV × 100 GeV eD, 36.8 fb^{-1}	P2	5 GeV × 100 GeV ep, 36.8 fb^{-1}
D3	10 GeV × 100 GeV eD, 44.8 fb^{-1}	P3	10 GeV × 100 GeV ep, 44.8 fb^{-1}
D4	10 GeV × 137 GeV eD, 100 fb^{-1}	P4	10 GeV × 275 GeV ep, 100 fb^{-1}
D5	18 GeV × 137 GeV eD, 15.4 fb^{-1}	P5	18 GeV × 275 GeV ep, 15.4 fb^{-1}
		P6	18 GeV × 275 GeV ep, 100 fb^{-1}

[Boughezal, Emmert, Kutz, SM, Nycz, Petriello, Simsek, Wiegand, Zheng]

- Projections for weak mixing angle extraction at the EIC from electron-proton PVDIS.

Beam type and energy Label	ep 5 × 100 P2	ep 10 × 100 P3	ep 10 × 275 P4	ep 18 × 275 P5	ep 18 × 275 P6
Luminosity (fb^{-1})	36.8	44.8	100	15.4	(100 YR ref)
$\langle Q^2\rangle$ (GeV^2)	154.4	308.1	687.3	1055.1	1055.1
$\langle A_{PV}\rangle$ ($P_e = 0.8$)	−0.00854	−0.01617	−0.03254	−0.04594	−0.04594
$(\mathrm{d}A/A)_{\text{stat}}$	1.54%	0.98%	0.40%	0.80%	(0.31%)
$(\mathrm{d}A/A)_{\text{stat+syst(bg)}}$	1.55%	1.00%	0.43%	0.81%	(0.35%)
$(\mathrm{d}A/A)_{1\%\text{pol}}$	1.0%	1.0%	1.0%	1.0%	(1.0%)
$(\mathrm{d}A/A)_{\text{tot}}$	1.84%	1.42%	1.09%	1.29%	(1.06%)
Experimental					
$\mathrm{d}(\sin^2\theta_W)_{\text{stat+syst(bg)}}$	0.002032	0.001299	0.000597	0.001176	0.000516
$\mathrm{d}(\sin^2\theta_W)_{\text{stat+syst+pol}}$	0.002342	0.001759	0.001297	0.001769	0.001244
with PDF					
$\mathrm{d}(\sin^2\theta_W)_{\text{tot,CT18NLO}}$	0.002388	0.001807	0.001363	0.001823	0.001320
$\mathrm{d}(\sin^2\theta_W)_{\text{tot,MMHT2014}}$	0.002353	0.001771	0.001319	0.001781	0.001270
$\mathrm{d}(\sin^2\theta_W)_{\text{tot,NNPDF31}}$	0.002351	0.001789	0.001313	0.001801	0.001308

TABLE III. Projected PVDIS asymmetry and fitted results for $\sin^2\theta_W$ using ep collision data and the nominal annual luminosity. Here, $\langle Q^2\rangle$ denotes the value averaged over all (x, Q^2) bins, weighted by $(\mathrm{d}A/A)^{-2}_{\text{stat}}$ for each bin. The electron beam polarization is assumed to be 80% with a relative 1% uncertainty. The total ("tot") uncertainty is from combining all of statistical, 1% systematic (background), 1% beam polarization, and PDF uncertainties evaluated using three different PDF sets. The rightmost column is for comparison with the YR.

- Projections for weak mixing angle extraction at the EIC from electron-deuteron PVDIS.

Beam type and energy Label	eD 5 × 100 D2	eD 10 × 100 D3	eD 10 × 137 D4	eD 18 × 137 D5	eD 18 × 137 N/A
Luminosity (fb^{-1})	36.8	44.8	100	15.4	(10 YR ref)
$\langle Q^2\rangle$ (GeV^2)	160.0	316.9	403.5	687.2	687.2
$\langle A_{PV}\rangle$ ($P_e = 0.8$)	−0.01028	−0.01923	−0.02366	−0.03719	−0.03719
$(\mathrm{d}A/A)_{\text{stat}}$	1.46%	0.93%	0.54%	1.05%	(1.31%)
$(\mathrm{d}A/A)_{\text{stat+bg}}$	1.47%	0.95%	0.56%	1.07%	(1.32%)
$(\mathrm{d}A/A)_{\text{syst},1\%\text{pol}}$	1.0%	1.0%	1.0%	1.0%	(1.0%)
$(\mathrm{d}A/A)_{\text{tot}}$	1.78%	1.38%	1.15%	1.46%	(1.66%)
Experimental					
$\mathrm{d}(\sin^2\theta_W)_{\text{stat+bg}}$	0.002148	0.001359	0.000823	0.001591	0.001963
$\mathrm{d}(\sin^2\theta_W)_{\text{stat+bg+pol}}$	0.002515	0.001904	0.001544	0.002116	0.002414
with PDF					
$\mathrm{d}(\sin^2\theta_W)_{\text{tot,CT18}}$	0.002558	0.001936	0.001566	0.002173	0.00247
$\mathrm{d}(\sin^2\theta_W)_{\text{tot,MMHT2014}}$	0.002527	0.001917	0.001562	0.002128	0.002424
$\mathrm{d}(\sin^2\theta_W)_{\text{tot,NNPDF31}}$	0.002526	0.001915	0.001560	0.002127	0.002423

TABLE IV. Projected PVDIS asymmetry and fitted results for $\sin^2\theta_W$ using eD collision data and the nominal annual luminosity. The uncertainty evaluation is the same as Table III.

SMEFT Analysis

Standard Model Effective Theory (SMEFT) Operator Basis

[Boughazel, Petriello, Wiegand]

- The SMEFT basis often used in global fit analysis to constrain new physics beyond the electroweak scale:

$$\mathcal{L} = \mathcal{L}_{SM} + \frac{1}{\Lambda^2}\sum_i C_i^6 \mathcal{O}_{6,i} + \frac{1}{\Lambda^4}\sum_i C_i^8 \mathcal{O}_{8,i} + \dots$$

- Relevant SMEFT operators for DIS processes at dim-6 and dim-8

Dimension 6		Dimension 8	
$\mathcal{O}_{lq}^{(1)}$	$(\bar{l}\gamma^\mu l)\,(\bar{q}\gamma_\mu q)$	$\mathcal{O}_{l^2q^2D^2}^{(1)}$	$D^\nu\,(\bar{l}\gamma^\mu l)\,D_\nu\,(\bar{q}\gamma_\mu q)$
$\mathcal{O}_{lq}^{(3)}$	$(\bar{l}\gamma^\mu\tau^i l)\,(\bar{q}\gamma_\mu\tau^i q)$	$\mathcal{O}_{l^2q^2D^2}^{(3)}$	$D^\nu\,(\bar{l}\gamma^\mu\tau^i l)\,D_\nu\,(\bar{q}\gamma_\mu\tau^i q)$
$\mathcal{O}_{eu}$	$(\bar{e}\gamma^\mu e)\,(\bar{u}\gamma_\mu u)$	$\mathcal{O}_{e^2u^2D^2}^{(1)}$	$D^\nu\,(\bar{e}\gamma^\mu e)\,D_\nu\,(\bar{u}\gamma_\mu u)$
$\mathcal{O}_{ed}$	$(\bar{e}\gamma^\mu e)\,(\bar{d}\gamma_\mu d)$	$\mathcal{O}_{e^2d^2D^2}^{(1)}$	$D^\nu\,(\bar{e}\gamma^\mu e)\,D_\nu\,(\bar{d}\gamma_\mu d)$
$\mathcal{O}_{lu}$	$(\bar{l}\gamma^\mu l)\,(\bar{u}\gamma_\mu u)$	$\mathcal{O}_{l^2u^2D^2}^{(1)}$	$D^\nu\,(\bar{l}\gamma^\mu l)\,D_\nu\,(\bar{u}\gamma_\mu u)$
$\mathcal{O}_{ld}$	$(\bar{l}\gamma^\mu l)\,(\bar{d}\gamma_\mu d)$	$\mathcal{O}_{l^2d^2D^2}^{(1)}$	$D^\nu\,(\bar{l}\gamma^\mu l)\,D_\nu\,(\bar{d}\gamma_\mu d)$
$\mathcal{O}_{qe}$	$(\bar{q}\gamma^\mu q)\,(\bar{e}\gamma_\mu e)$	$\mathcal{O}_{q^2e^2D^2}^{(1)}$	$D^\nu\,(\bar{q}\gamma^\mu q)\,D_\nu\,(\bar{e}\gamma_\mu e)$

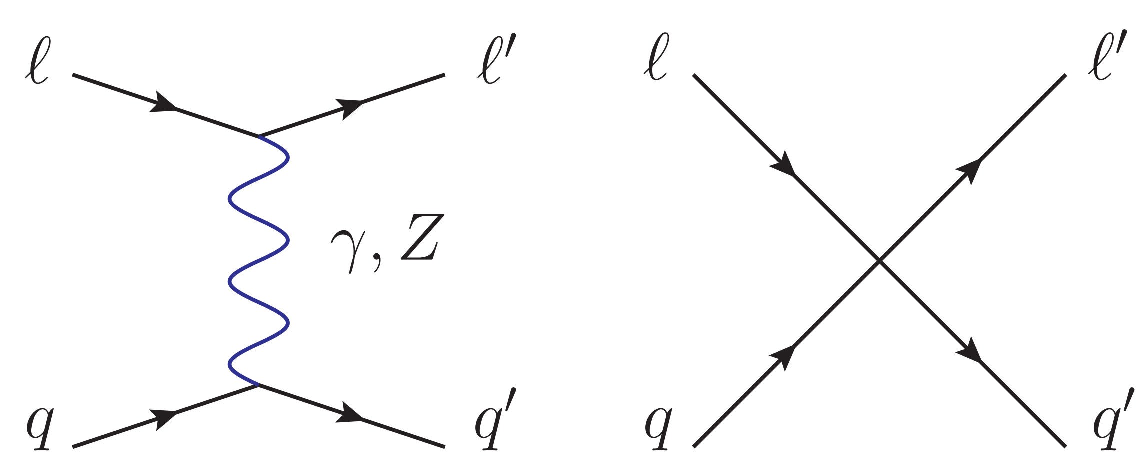

SMEFT vs C_{iq} Basis

[Boughazel, Petriello, Wiegand]

- For low energy experiments, typically the C_{iq} basis of operators based on V-A structure after EWSB is used:

$$\mathcal{L}_{PV} = \frac{G_F}{\sqrt{2}}\Big[(\bar{e}\gamma^\mu\gamma_5 e)(C^6_{1u}\bar{u}\gamma_\mu u + C^6_{1d}\bar{d}\gamma_\mu d) + (\bar{e}\gamma^\mu e)(C^6_{2u}\bar{u}\gamma_\mu\gamma_5 u + C^6_{2d}\bar{d}\gamma_\mu\gamma_5 d)$$
$$+ (\bar{e}\gamma^\mu e)(C^6_{Vu}\bar{u}\gamma_\mu u + C^6_{Vd}\bar{d}\gamma_\mu d) + (\bar{e}\gamma^\mu\gamma_5 e)(C^6_{Au}\bar{u}\gamma_\mu\gamma_5 u)$$
$$+ D^\nu\left(\bar{e}\gamma^\mu\gamma_5 e\right)D_\nu\left(\frac{C^8_{1u}}{v^2}\bar{u}\gamma_\mu u + \frac{C^8_{1d}}{v^2}\bar{d}\gamma_\mu d\right) + D^\nu\left(\bar{e}\gamma^\mu e\right)D_\nu\left(\frac{C^8_{2u}}{v^2}\bar{u}\gamma_\mu\gamma_5 u + \frac{C^8_{2d}}{v^2}\bar{d}\gamma_\mu\gamma_5 d\right)$$
$$+ D^\nu\left(\bar{e}\gamma^\mu e\right)D_\nu\left(\frac{C^8_{Vu}}{v^2}\bar{u}\gamma_\mu u + \frac{C^8_{Vd}}{v^2}\bar{d}\gamma_\mu d\right) + D^\nu\left(\bar{e}\gamma^\mu\gamma_5 e\right)D_\nu\left(\frac{C^8_{Au}}{v^2}\bar{u}\gamma_\mu\gamma_5 u\right)\Big].$$

- One can find relations between the two bases:

$$C^6_{1u} = 2(g^e_R - g^e_L)(g^u_R + g^u_L) + \frac{v^2}{2\Lambda^2}\left\{-\left(C^{(1)}_{lq} - C^{(3)}_{lq}\right) + C_{eu} + C_{qe} - C_{lu}\right\}$$
$$C^6_{2u} = 2(g^e_R + g^e_L)(g^u_R - g^u_L) + \frac{v^2}{2\Lambda^2}\left\{-\left(C^{(1)}_{lq} - C^{(3)}_{lq}\right) + C_{eu} - C_{qe} + C_{lu}\right\}$$
$$C^6_{1d} = 2(g^e_R - g^e_L)(g^d_R + g^d_L) + \frac{v^2}{2\Lambda^2}\left\{-\left(C^{(1)}_{lq} + C^{(3)}_{lq}\right) + C_{ed} + C_{qe} - C_{ld}\right\}$$
$$C^6_{2d} = 2(g^e_R + g^e_L)(g^d_R - g^d_L) + \frac{v^2}{2\Lambda^2}\left\{-\left(C^{(1)}_{lq} + C^{(3)}_{lq}\right) + C_{ed} - C_{qe} + C_{ld}\right\}$$
$$C^6_{Vu} = 2(g^e_R + g^e_L)(g^u_R + g^u_L) + \frac{v^2}{2\Lambda^2}\left\{\left(C^{(1)}_{lq} - C^{(3)}_{lq}\right) + C_{eu} + C_{qe} + C_{lu}\right\}$$
$$C^6_{Au} = 2(g^e_R - g^e_L)(g^u_R - g^u_L) + \frac{v^2}{2\Lambda^2}\left\{\left(C^{(1)}_{lq} - C^{(3)}_{lq}\right) + C_{eu} - C_{qe} - C_{lu}\right\}$$
$$C^6_{Vd} = 2(g^e_R + g^e_L)(g^d_R + g^d_L) + \frac{v^2}{2\Lambda^2}\left\{\left(C^{(1)}_{lq} + C^{(3)}_{lq}\right) + C_{ed} + C_{qe} + C_{ld}\right\}.$$

SMEFT Constraints from Drell-Yan at LHC

[Boughazel, Petriello, Wiegand]

- The SMEFT Wilson coefficients that affect PVES also contribute to the Drell-Yan process at the LHC

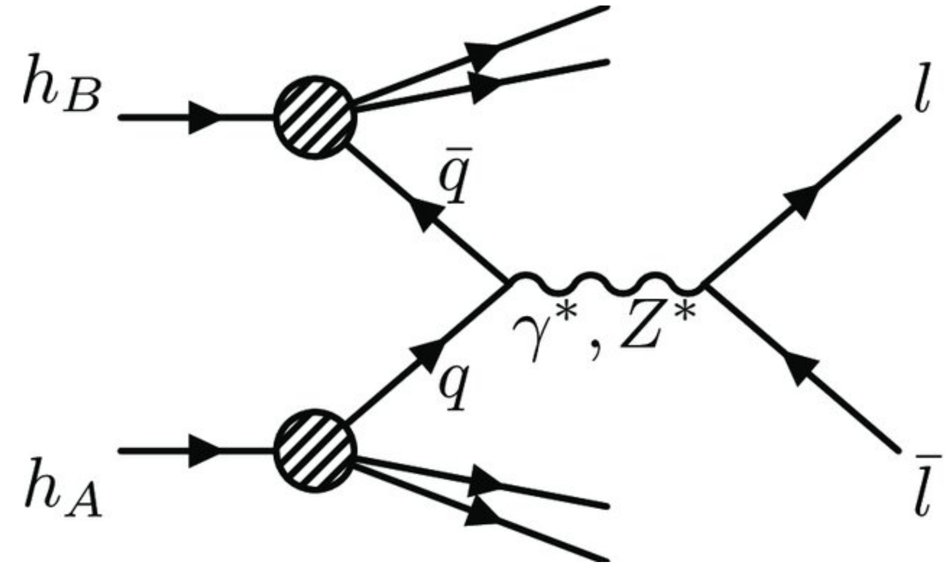

$$\frac{d\sigma_{q\bar{q}}}{dm_{ll}^2 dY dc_\theta} = \frac{1}{32\pi m_{ll}^2 \hat{s}} f_q(x_1) f_{\bar{q}}(x_2) \left\{ \frac{d\hat{\sigma}_{q\bar{q}}^{\gamma\gamma}}{dm_{ll}^2 dY dc_\theta} + \frac{d\hat{\sigma}_{q\bar{q}}^{\gamma Z}}{dm_{ll}^2 dY dc_\theta} + \frac{d\hat{\sigma}_{q\bar{q}}^{ZZ}}{dm_{ll}^2 dY dc_\theta} \right.$$
$$\left. + \frac{d\hat{\sigma}_{q\bar{q}}^{\gamma SMEFT6}}{dm_{ll}^2 dY dc_\theta} + \frac{d\hat{\sigma}_{q\bar{q}}^{Z SMEFT6}}{dm_{ll}^2 dY dc_\theta} + \frac{d\hat{\sigma}_{q\bar{q}}^{\gamma SMEFT8}}{dm_{ll}^2 dY dc_\theta} + \frac{d\hat{\sigma}_{q\bar{q}}^{Z SMEFT8}}{dm_{ll}^2 dY dc_\theta} + \frac{d\hat{\sigma}_{q\bar{q}}^{SMEFT6^2}}{dm_{ll}^2 dY dc_\theta} \right\}$$

- PVES and the LHC can be complementary to each other in constraining new physics

Constraining BSM and Lifting Flat Directions

[Boughezal, Emmert, Kutz, SM, Nycz, Petriello, Simsek, Wiegand, Zheng]

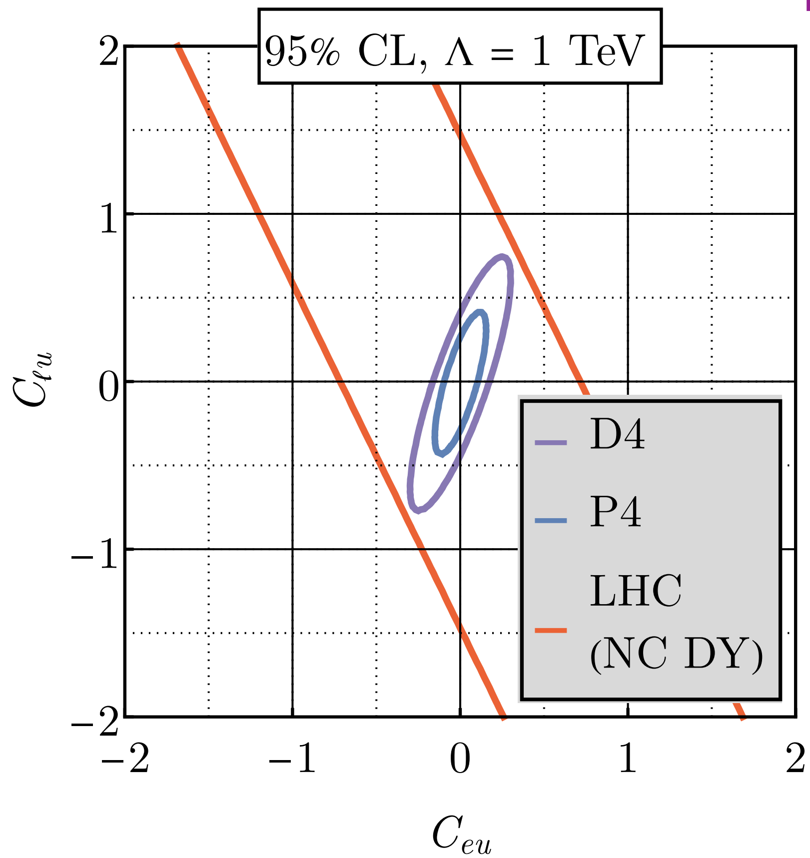

- PVDIS and Drell-Yan at the LHC are sensitive to different combinations of the SMEFT Wilson coefficients.

- PVDIS can lift "flat directions" by probing orthogonal directions in the SMEFT parameter space compared to the LHC

Dimension 6		Dimension 8	
$\mathcal{O}_{lq}^{(1)}$	$(\bar{l}\gamma^\mu l)\,(\bar{q}\gamma_\mu q)$	$\mathcal{O}_{l^2q^2D^2}^{(1)}$	$D^\nu\,(\bar{l}\gamma^\mu l)\,D_\nu\,(\bar{q}\gamma_\mu q)$
$\mathcal{O}_{lq}^{(3)}$	$(\bar{l}\gamma^\mu\tau^i l)\,(\bar{q}\gamma_\mu\tau^i q)$	$\mathcal{O}_{l^2q^2D^2}^{(3)}$	$D^\nu\,(\bar{l}\gamma^\mu\tau^i l)\,D_\nu\,(\bar{q}\gamma_\mu\tau^i q)$
$\mathcal{O}_{eu}$	$(\bar{e}\gamma^\mu e)\,(\bar{u}\gamma_\mu u)$	$\mathcal{O}_{e^2u^2D^2}^{(1)}$	$D^\nu\,(\bar{e}\gamma^\mu e)\,D_\nu\,(\bar{u}\gamma_\mu u)$
$\mathcal{O}_{ed}$	$(\bar{e}\gamma^\mu e)\,(\bar{d}\gamma_\mu d)$	$\mathcal{O}_{e^2d^2D^2}^{(1)}$	$D^\nu\,(\bar{e}\gamma^\mu e)\,D_\nu\,(\bar{d}\gamma_\mu d)$
$\mathcal{O}_{lu}$	$(\bar{l}\gamma^\mu l)\,(\bar{u}\gamma_\mu u)$	$\mathcal{O}_{l^2u^2D^2}^{(1)}$	$D^\nu\,(\bar{l}\gamma^\mu l)\,D_\nu\,(\bar{u}\gamma_\mu u)$
$\mathcal{O}_{ld}$	$(\bar{l}\gamma^\mu l)\,(\bar{d}\gamma_\mu d)$	$\mathcal{O}_{l^2d^2D^2}^{(1)}$	$D^\nu\,(\bar{l}\gamma^\mu l)\,D_\nu\,(\bar{d}\gamma_\mu d)$
$\mathcal{O}_{qe}$	$(\bar{q}\gamma^\mu q)\,(\bar{e}\gamma_\mu e)$	$\mathcal{O}_{q^2e^2D^2}^{(1)}$	$D^\nu\,(\bar{q}\gamma^\mu q)\,D_\nu\,(\bar{e}\gamma_\mu e)$

D1	5 GeV × 41 GeV eD, 4.4 fb^{-1}	P1	5 GeV × 41 GeV ep, 4.4 fb^{-1}
D2	5 GeV × 100 GeV eD, 36.8 fb^{-1}	P2	5 GeV × 100 GeV ep, 36.8 fb^{-1}
D3	10 GeV × 100 GeV eD, 44.8 fb^{-1}	P3	10 GeV × 100 GeV ep, 44.8 fb^{-1}
D4	10 GeV × 137 GeV eD, 100 fb^{-1}	P4	10 GeV × 275 GeV ep, 100 fb^{-1}
D5	18 GeV × 137 GeV eD, 15.4 fb^{-1}	P5	18 GeV × 275 GeV ep, 15.4 fb^{-1}
		P6	18 GeV × 275 GeV ep, 100 fb^{-1}

Constraining BSM and Lifting Flat Directions

[Boughezal, Emmert, Kutz, SM, Nycz, Petriello, Simsek, Wiegand, Zheng]

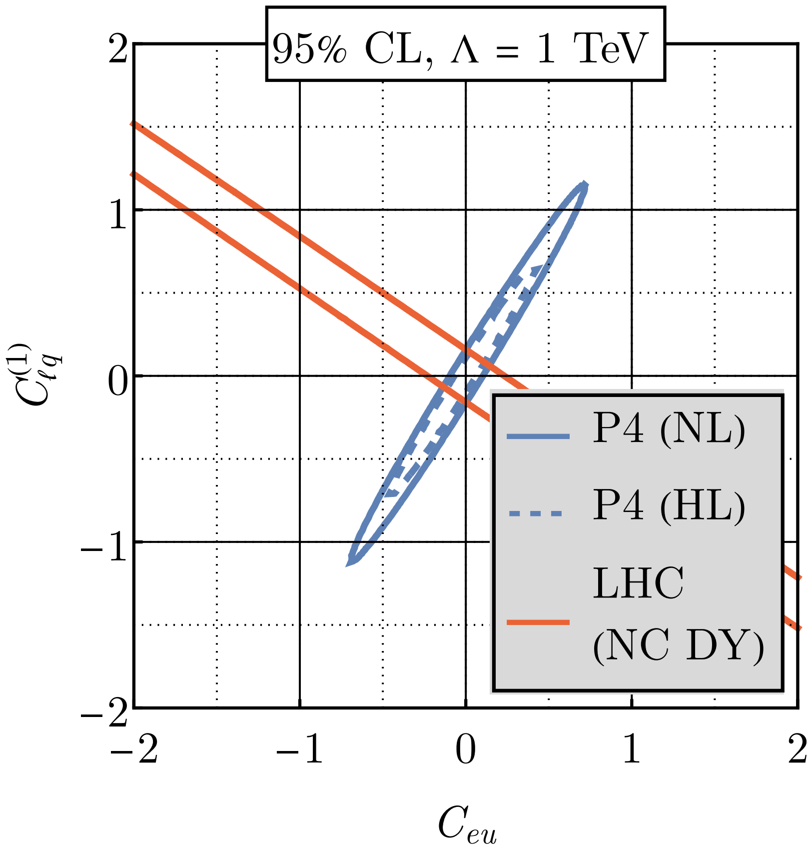

Dimension 6		Dimension 8	
$\mathcal{O}_{lq}^{(1)}$	$(\bar{l}\gamma^\mu l)\,(\bar{q}\gamma_\mu q)$	$\mathcal{O}_{l^2q^2D^2}^{(1)}$	$D^\nu\,(\bar{l}\gamma^\mu l)\,D_\nu\,(\bar{q}\gamma_\mu q)$
$\mathcal{O}_{lq}^{(3)}$	$(\bar{l}\gamma^\mu\tau^i l)\,(\bar{q}\gamma_\mu\tau^i q)$	$\mathcal{O}_{l^2q^2D^2}^{(3)}$	$D^\nu\,(\bar{l}\gamma^\mu\tau^i l)\,D_\nu\,(\bar{q}\gamma_\mu\tau^i q)$
$\mathcal{O}_{eu}$	$(\bar{e}\gamma^\mu e)\,(\bar{u}\gamma_\mu u)$	$\mathcal{O}_{e^2u^2D^2}^{(1)}$	$D^\nu\,(\bar{e}\gamma^\mu e)\,D_\nu\,(\bar{u}\gamma_\mu u)$
$\mathcal{O}_{ed}$	$(\bar{e}\gamma^\mu e)\,(\bar{d}\gamma_\mu d)$	$\mathcal{O}_{e^2d^2D^2}^{(1)}$	$D^\nu\,(\bar{e}\gamma^\mu e)\,D_\nu\,(\bar{d}\gamma_\mu d)$
$\mathcal{O}_{lu}$	$(\bar{l}\gamma^\mu l)\,(\bar{u}\gamma_\mu u)$	$\mathcal{O}_{l^2u^2D^2}^{(1)}$	$D^\nu\,(\bar{l}\gamma^\mu l)\,D_\nu\,(\bar{u}\gamma_\mu u)$
$\mathcal{O}_{ld}$	$(\bar{l}\gamma^\mu l)\,(\bar{d}\gamma_\mu d)$	$\mathcal{O}_{l^2d^2D^2}^{(1)}$	$D^\nu\,(\bar{l}\gamma^\mu l)\,D_\nu\,(\bar{d}\gamma_\mu d)$
$\mathcal{O}_{qe}$	$(\bar{q}\gamma^\mu q)\,(\bar{e}\gamma_\mu e)$	$\mathcal{O}_{q^2e^2D^2}^{(1)}$	$D^\nu\,(\bar{q}\gamma^\mu q)\,D_\nu\,(\bar{e}\gamma_\mu e)$

- PVDIS and Drell-Yan at the LHC are sensitive to different combinations of the SMEFT Wilson coefficients.

- PVDIS can lift "flat directions" by probing orthogonal directions in the SMEFT parameter space compared to the LHC

D1	5 GeV × 41 GeV eD, 4.4 fb^{-1}	P1	5 GeV × 41 GeV ep, 4.4 fb^{-1}
D2	5 GeV × 100 GeV eD, 36.8 fb^{-1}	P2	5 GeV × 100 GeV ep, 36.8 fb^{-1}
D3	10 GeV × 100 GeV eD, 44.8 fb^{-1}	P3	10 GeV × 100 GeV ep, 44.8 fb^{-1}
D4	10 GeV × 137 GeV eD, 100 fb^{-1}	P4	10 GeV × 275 GeV ep, 100 fb^{-1}
D5	18 GeV × 137 GeV eD, 15.4 fb^{-1}	P5	18 GeV × 275 GeV ep, 15.4 fb^{-1}
		P6	18 GeV × 275 GeV ep, 100 fb^{-1}

Constraining BSM and Lifting Flat Directions

[Boughezal, Emmert, Kutz, SM, Nycz, Petriello, Simsek, Wiegand, Zheng]

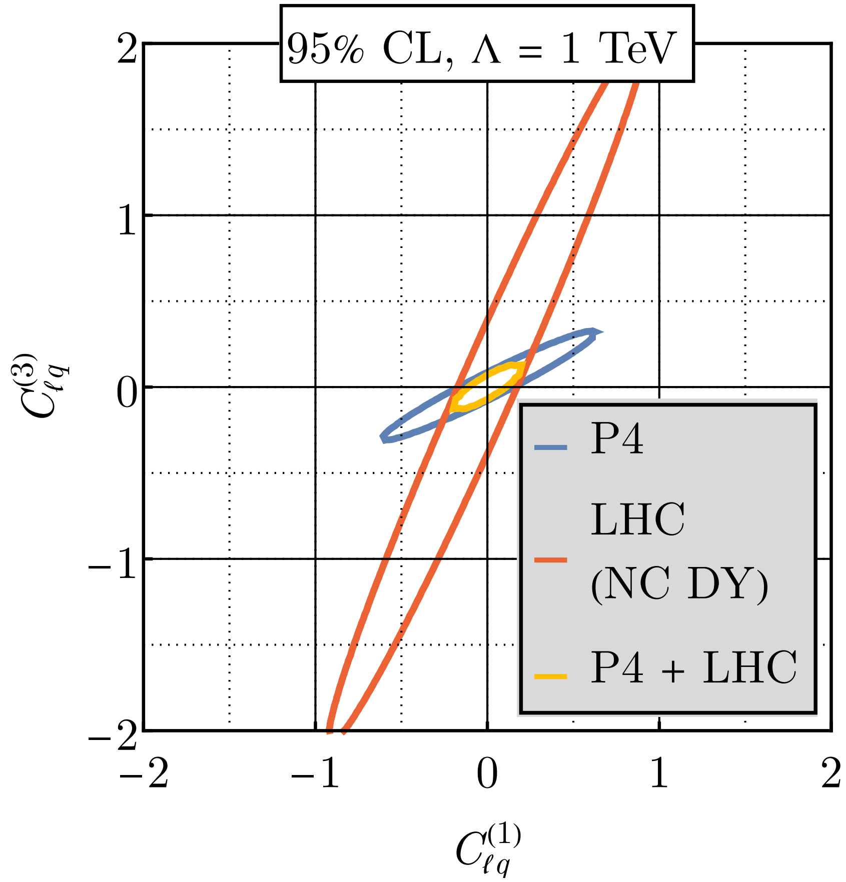

- PVDIS and Drell-Yan at the LHC are sensitive to different combinations of the SMEFT Wilson coefficients.

- PVDIS can lift "flat directions" by probing orthogonal directions in the SMEFT parameter space compared to the LHC

Dimension 6		Dimension 8	
$\mathcal{O}_{lq}^{(1)}$	$(\bar{l}\gamma^{\mu}l)\,(\bar{q}\gamma_{\mu}q)$	$\mathcal{O}_{l^2q^2D^2}^{(1)}$	$D^{\nu}\,(\bar{l}\gamma^{\mu}l)\,D_{\nu}\,(\bar{q}\gamma_{\mu}q)$
$\mathcal{O}_{lq}^{(3)}$	$(\bar{l}\gamma^{\mu}\tau^{i}l)\,(\bar{q}\gamma_{\mu}\tau^{i}q)$	$\mathcal{O}_{l^2q^2D^2}^{(3)}$	$D^{\nu}\,(\bar{l}\gamma^{\mu}\tau^{i}l)\,D_{\nu}\,(\bar{q}\gamma_{\mu}\tau^{i}q)$
$\mathcal{O}_{eu}$	$(\bar{e}\gamma^{\mu}e)\,(\bar{u}\gamma_{\mu}u)$	$\mathcal{O}_{e^2u^2D^2}^{(1)}$	$D^{\nu}\,(\bar{e}\gamma^{\mu}e)\,D_{\nu}\,(\bar{u}\gamma_{\mu}u)$
$\mathcal{O}_{ed}$	$(\bar{e}\gamma^{\mu}e)\,(\bar{d}\gamma_{\mu}d)$	$\mathcal{O}_{e^2d^2D^2}^{(1)}$	$D^{\nu}\,(\bar{e}\gamma^{\mu}e)\,D_{\nu}\,(\bar{d}\gamma_{\mu}d)$
$\mathcal{O}_{lu}$	$(\bar{l}\gamma^{\mu}l)\,(\bar{u}\gamma_{\mu}u)$	$\mathcal{O}_{l^2u^2D^2}^{(1)}$	$D^{\nu}\,(\bar{l}\gamma^{\mu}l)\,D_{\nu}\,(\bar{u}\gamma_{\mu}u)$
$\mathcal{O}_{ld}$	$(\bar{l}\gamma^{\mu}l)\,(\bar{d}\gamma_{\mu}d)$	$\mathcal{O}_{l^2d^2D^2}^{(1)}$	$D^{\nu}\,(\bar{l}\gamma^{\mu}l)\,D_{\nu}\,(\bar{d}\gamma_{\mu}d)$
$\mathcal{O}_{qe}$	$(\bar{q}\gamma^{\mu}q)\,(\bar{e}\gamma_{\mu}e)$	$\mathcal{O}_{q^2e^2D^2}^{(1)}$	$D^{\nu}\,(\bar{q}\gamma^{\mu}q)\,D_{\nu}\,(\bar{e}\gamma_{\mu}e)$

D1	5 GeV × 41 GeV eD, 4.4 fb^{-1}	P1	5 GeV × 41 GeV ep, 4.4 fb^{-1}
D2	5 GeV × 100 GeV eD, 36.8 fb^{-1}	P2	5 GeV × 100 GeV ep, 36.8 fb^{-1}
D3	10 GeV × 100 GeV eD, 44.8 fb^{-1}	P3	10 GeV × 100 GeV ep, 44.8 fb^{-1}
D4	10 GeV × 137 GeV eD, 100 fb^{-1}	P4	10 GeV × 275 GeV ep, 100 fb^{-1}
D5	18 GeV × 137 GeV eD, 15.4 fb^{-1}	P5	18 GeV × 275 GeV ep, 15.4 fb^{-1}
		P6	18 GeV × 275 GeV ep, 100 fb^{-1}

Constraining BSM and Lifting Flat Directions

[Boughezal, Emmert, Kutz, SM, Nycz, Petriello, Simsek, Wiegand, Zheng]

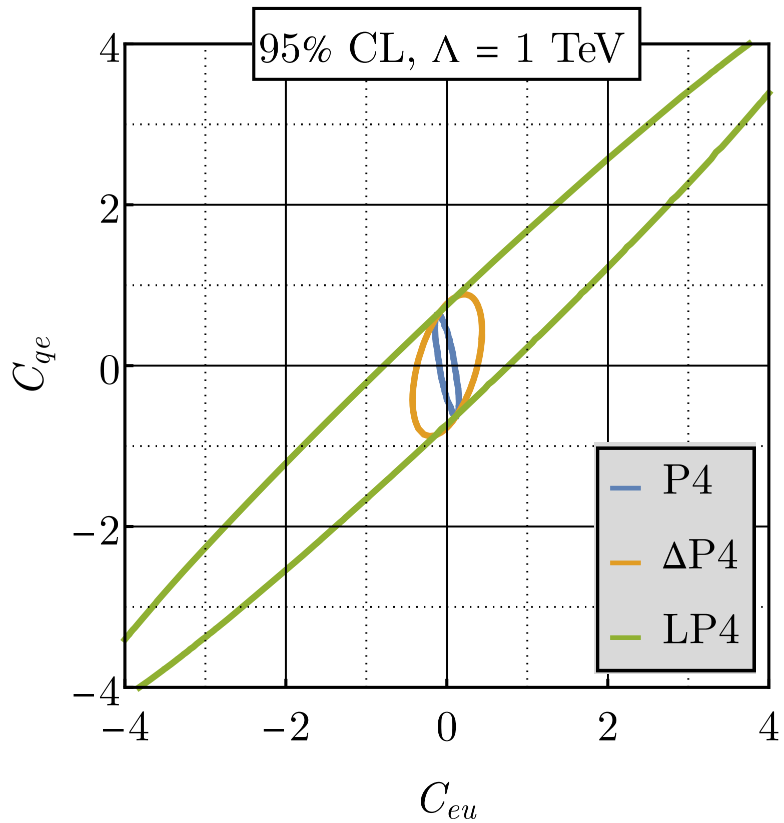

- PVDIS and Drell-Yan at the LHC are sensitive to different combinations of the SMEFT Wilson coefficients.

- PVDIS can lift "flat directions" by probing orthogonal directions in the SMEFT parameter space compared to the LHC

Dimension 6		Dimension 8	
$\mathcal{O}_{lq}^{(1)}$	$(\bar{l}\gamma^{\mu}l)\,(\bar{q}\gamma_{\mu}q)$	$\mathcal{O}_{l^2q^2D^2}^{(1)}$	$D^{\nu}\,(\bar{l}\gamma^{\mu}l)\,D_{\nu}\,(\bar{q}\gamma_{\mu}q)$
$\mathcal{O}_{lq}^{(3)}$	$(\bar{l}\gamma^{\mu}\tau^{i}l)\,(\bar{q}\gamma_{\mu}\tau^{i}q)$	$\mathcal{O}_{l^2q^2D^2}^{(3)}$	$D^{\nu}\,(\bar{l}\gamma^{\mu}\tau^{i}l)\,D_{\nu}\,(\bar{q}\gamma_{\mu}\tau^{i}q)$
$\mathcal{O}_{eu}$	$(\bar{e}\gamma^{\mu}e)\,(\bar{u}\gamma_{\mu}u)$	$\mathcal{O}_{e^2u^2D^2}^{(1)}$	$D^{\nu}\,(\bar{e}\gamma^{\mu}e)\,D_{\nu}\,(\bar{u}\gamma_{\mu}u)$
$\mathcal{O}_{ed}$	$(\bar{e}\gamma^{\mu}e)\,(\bar{d}\gamma_{\mu}d)$	$\mathcal{O}_{e^2d^2D^2}^{(1)}$	$D^{\nu}\,(\bar{e}\gamma^{\mu}e)\,D_{\nu}\,(\bar{d}\gamma_{\mu}d)$
$\mathcal{O}_{lu}$	$(\bar{l}\gamma^{\mu}l)\,(\bar{u}\gamma_{\mu}u)$	$\mathcal{O}_{l^2u^2D^2}^{(1)}$	$D^{\nu}\,(\bar{l}\gamma^{\mu}l)\,D_{\nu}\,(\bar{u}\gamma_{\mu}u)$
$\mathcal{O}_{ld}$	$(\bar{l}\gamma^{\mu}l)\,(\bar{d}\gamma_{\mu}d)$	$\mathcal{O}_{l^2d^2D^2}^{(1)}$	$D^{\nu}\,(\bar{l}\gamma^{\mu}l)\,D_{\nu}\,(\bar{d}\gamma_{\mu}d)$
$\mathcal{O}_{qe}$	$(\bar{q}\gamma^{\mu}q)\,(\bar{e}\gamma_{\mu}e)$	$\mathcal{O}_{q^2e^2D^2}^{(1)}$	$D^{\nu}\,(\bar{q}\gamma^{\mu}q)\,D_{\nu}\,(\bar{e}\gamma_{\mu}e)$

D1	5 GeV × 41 GeV *eD*, 4.4 fb^{-1}	P1	5 GeV × 41 GeV *ep*, 4.4 fb^{-1}
D2	5 GeV × 100 GeV *eD*, 36.8 fb^{-1}	P2	5 GeV × 100 GeV *ep*, 36.8 fb^{-1}
D3	10 GeV × 100 GeV *eD*, 44.8 fb^{-1}	P3	10 GeV × 100 GeV *ep*, 44.8 fb^{-1}
D4	10 GeV × 137 GeV *eD*, 100 fb^{-1}	P4	10 GeV × 275 GeV *ep*, 100 fb^{-1}
D5	18 GeV × 137 GeV *eD*, 15.4 fb^{-1}	P5	18 GeV × 275 GeV *ep*, 15.4 fb^{-1}
		P6	18 GeV × 275 GeV *ep*, 100 fb^{-1}

Disentangling Dim-6 and Dim-8 SMEFT Operators

[Boughezal, Petriello, Wiegand]

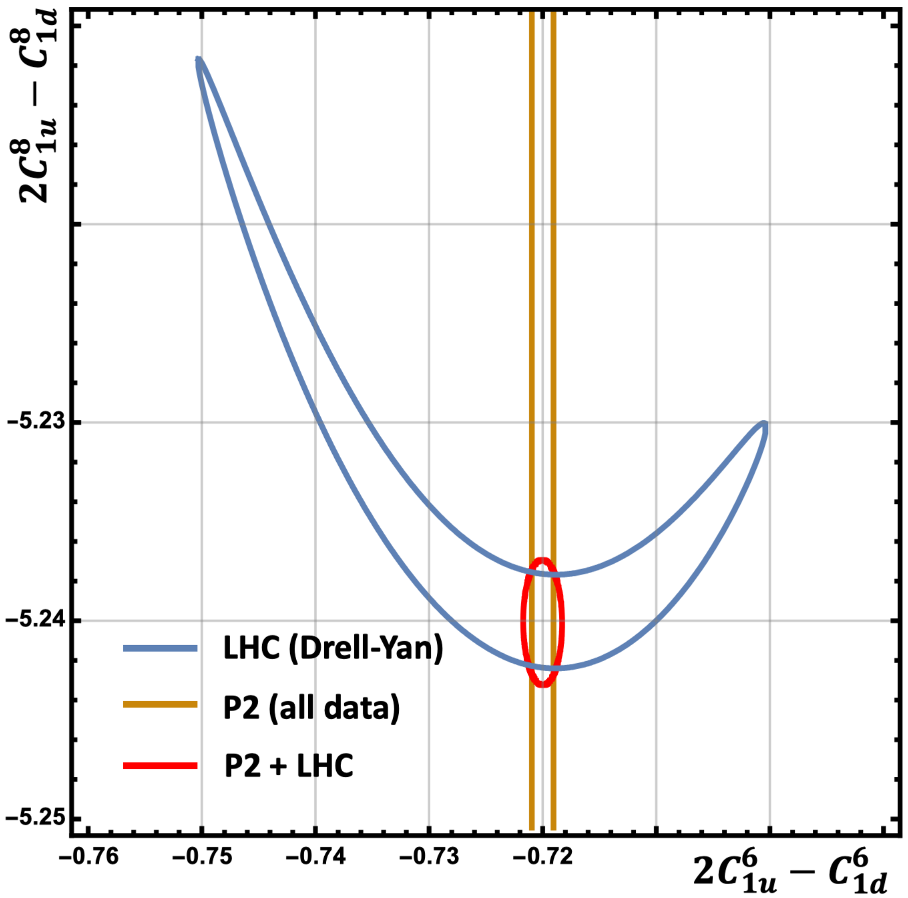

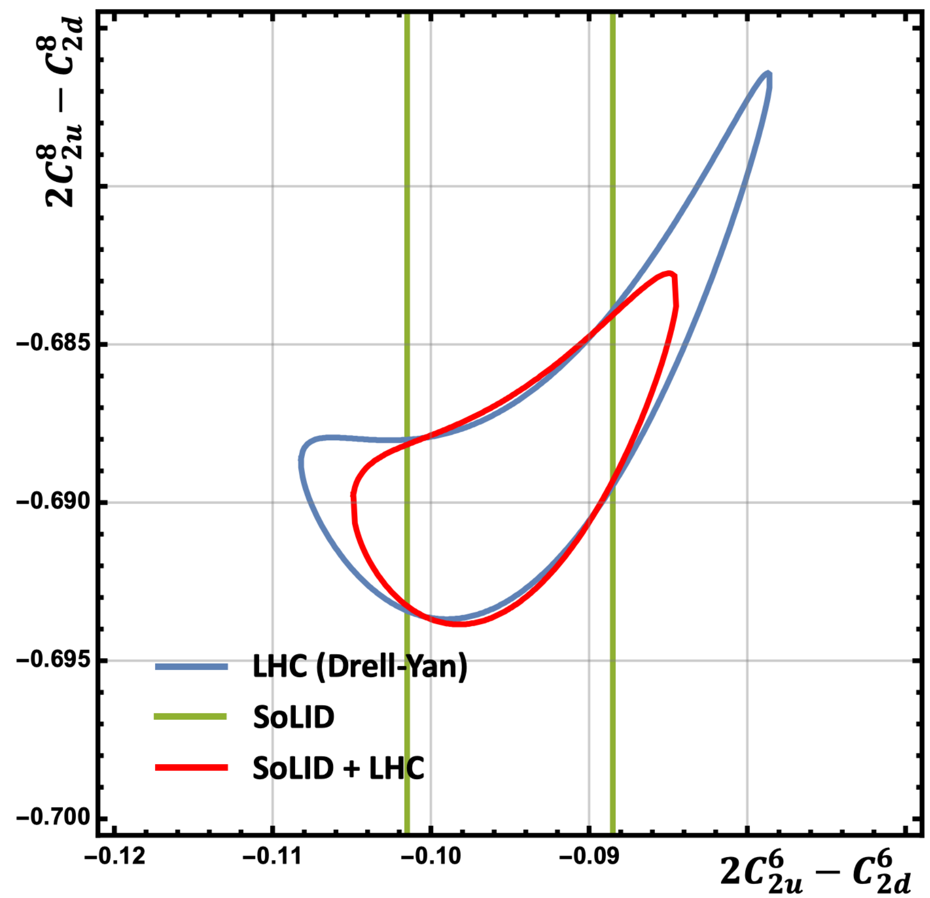

- Another advantage of low energy PVES experiments:

The large energy of the LHC can make it difficult to disentangle the effects of dim-6 or dim-8 (and dim-6 squared) operators.

Low energy PVES will only have sensitivity to dim-6 operators providing valuable input to disentangle dim-6 vs dim-8.

This is also true at the EIC

Electroweak Spin Structure Functions

Electroweak DIS

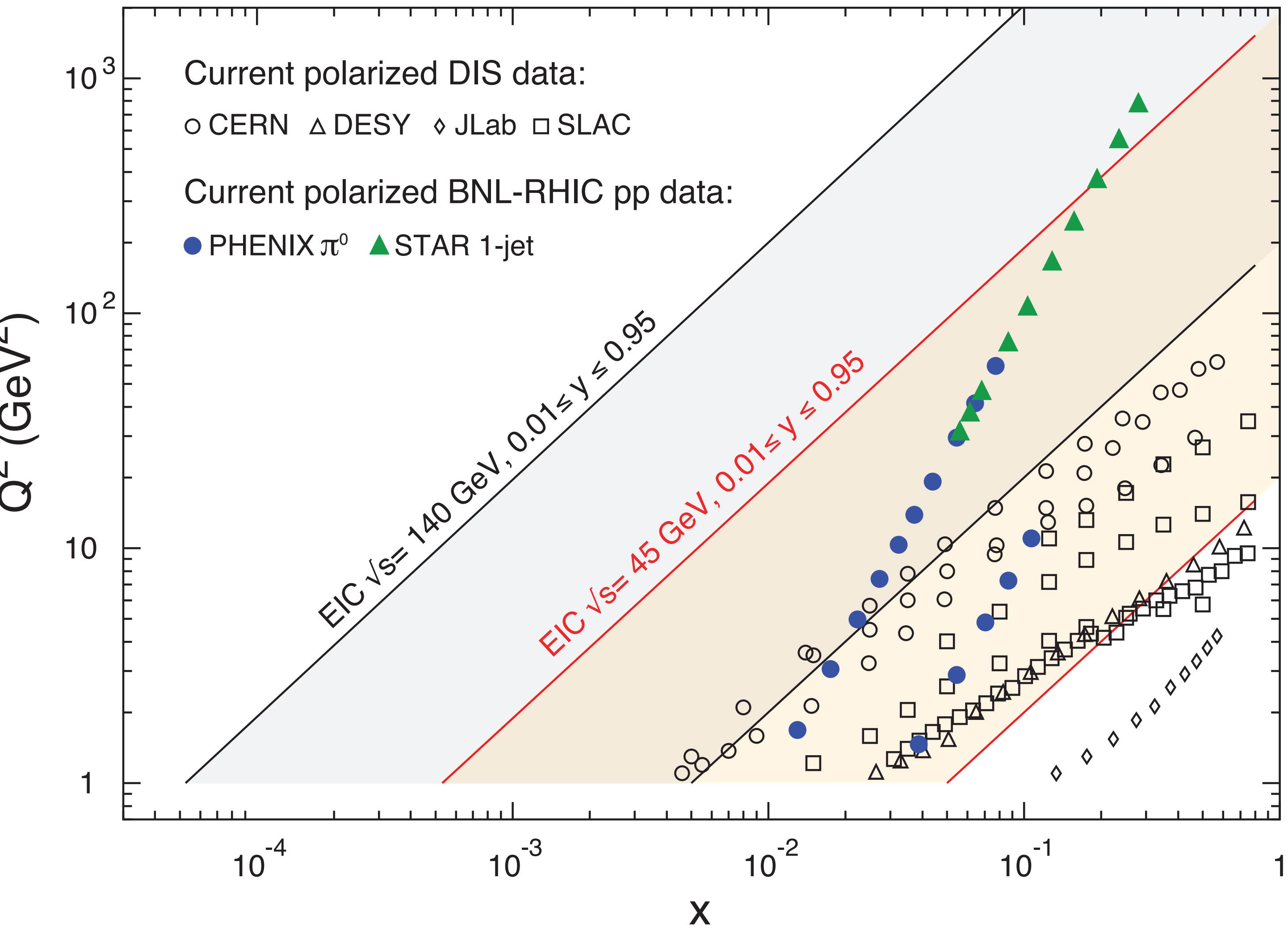

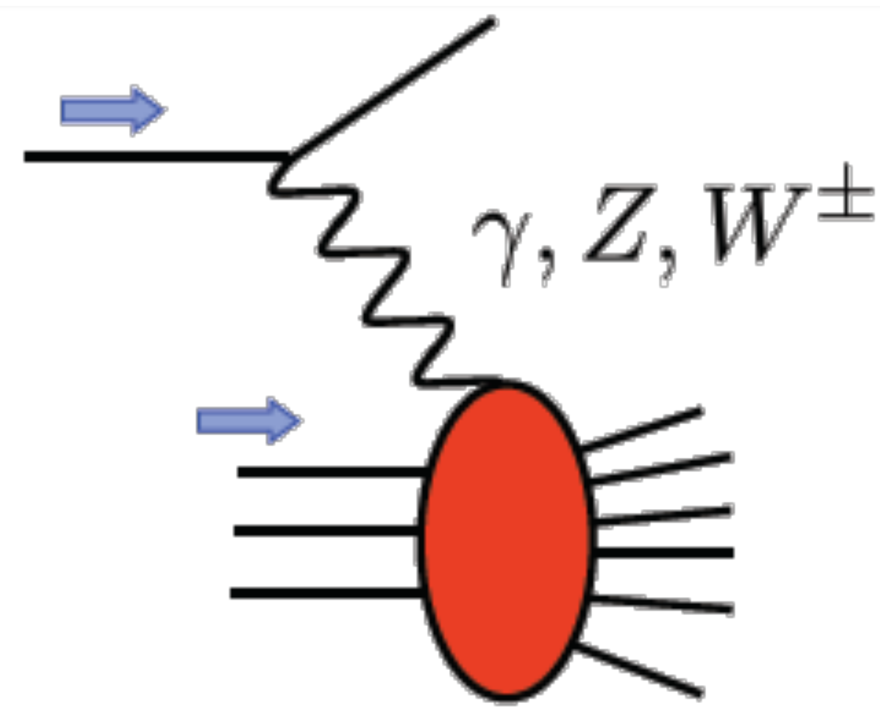

- The $\gamma, Z, W^{\pm}$ electroweak probes each probe different flavor combinations of nucleon structure functions, allowing for flavor separation.

  -NC DIS γ, Z exchange + interference

  -CC DIS W exchange

NC Target-flip Parity-Violating Asymmetry

- Polarized beam ion beams at EIC provide a new direction for exploring the nucleon spin structure:

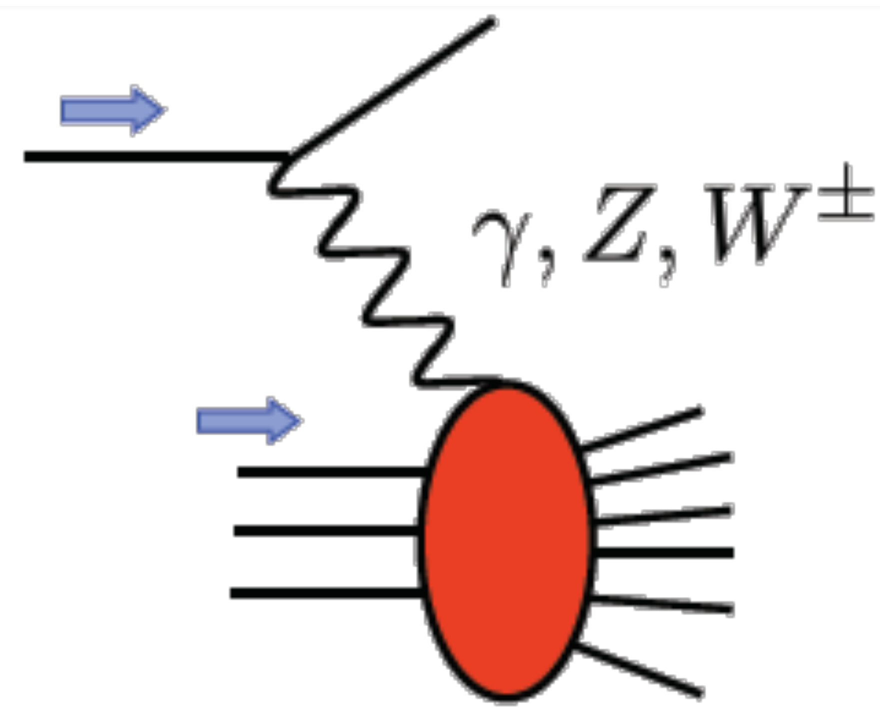

- NC DIS asymmetry:

$$g_1^{\gamma Z} = \sum e_q (g_V)_q (\Delta q + \Delta \bar{q})$$

$$g_5^{\gamma Z} = \sum_q e_q (g_A)_q (\Delta q - \Delta \bar{q})$$

- CC DIS asymmetry:

$$\begin{aligned} g_1^{W^-,p}(x) &= \Delta u(x) + \Delta \bar{d}(x) + \Delta c(x) + \Delta \bar{s}(x)\ , \\ g_5^{W^-,p}(x) &= -\Delta u(x) + \Delta \bar{d}(x) - \Delta c(x) + \Delta \bar{s}(x) \end{aligned}$$

[See dedicated talk by de Florian]

[See EIC Simulation studies: Aschenauer, Burton, Martini, Spiesberger, Stratmann, Sassot]

Jet Charge

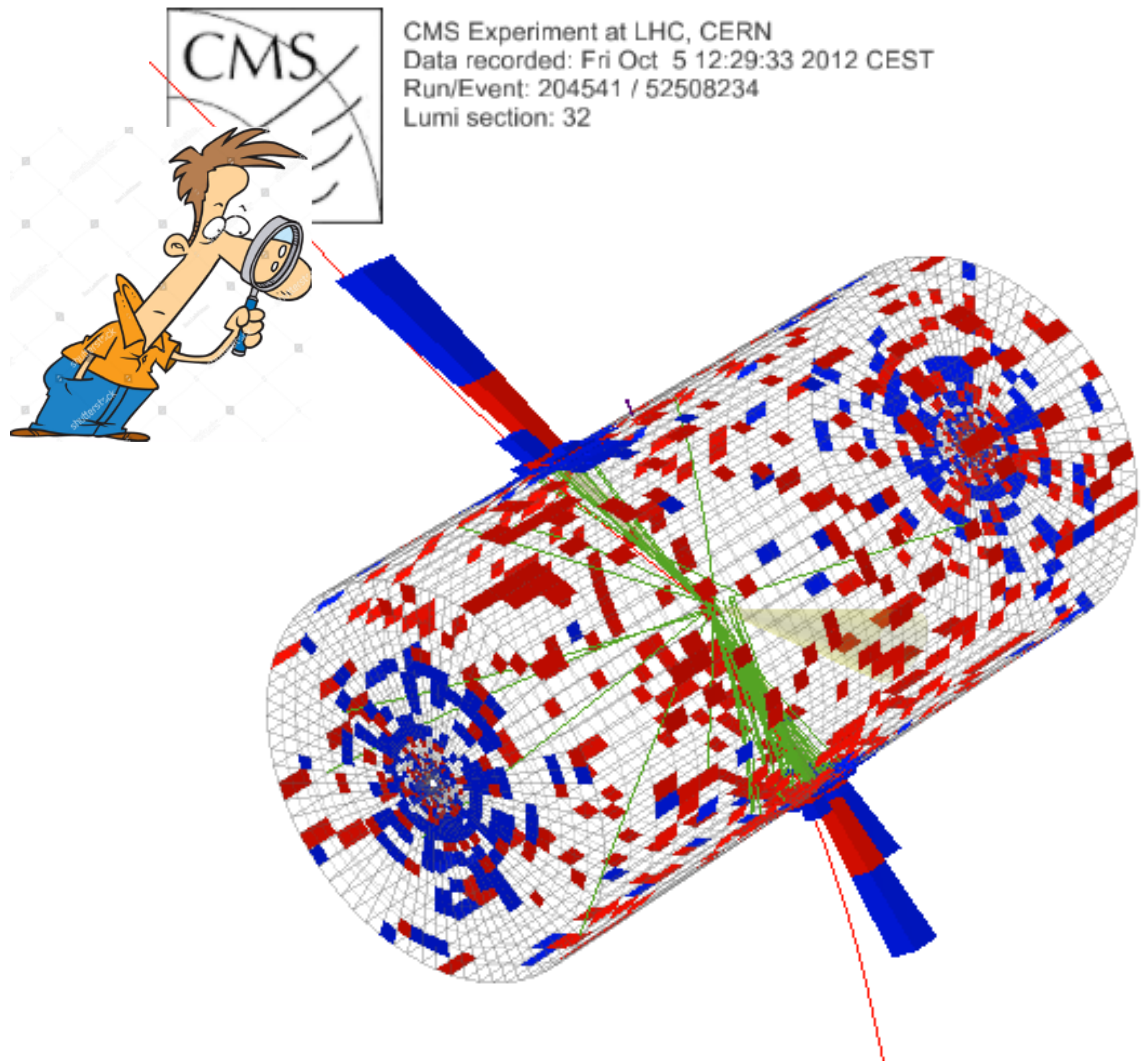
CMS Experiment at LHC, CERN
Data recorded: Fri Oct 5 12:29:33 2012 CEST
Run/Event: 204541 / 52508234
Lumi section: 32

Standard Jet Charge

[Feld, Feynman (1978); Krohn, Schwartz, Lin, Waalewijin (2012)]

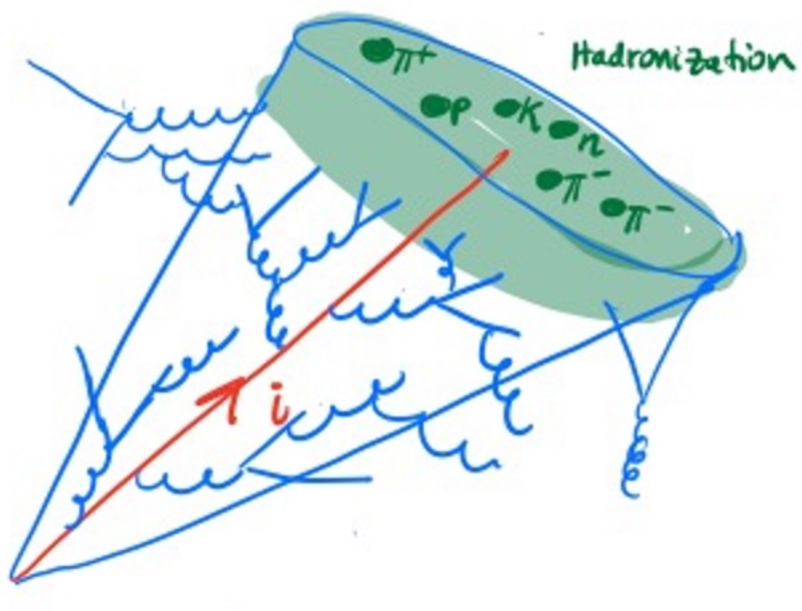

$$Q_\kappa^i = \sum_{h \in i\text{-jet}} z_h^\kappa \, Q_h$$

$$z_h = \frac{p_{T_h}}{p_{T_J}}$$

- Jet Charge can be used to discriminate jet flavor:

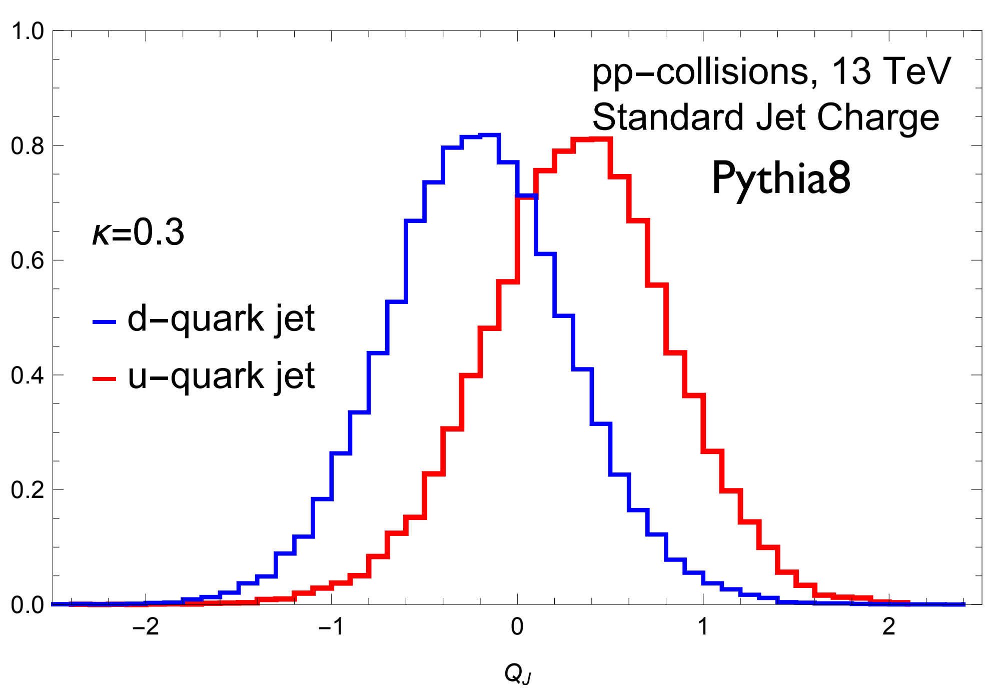

Good u vs. d discrimination

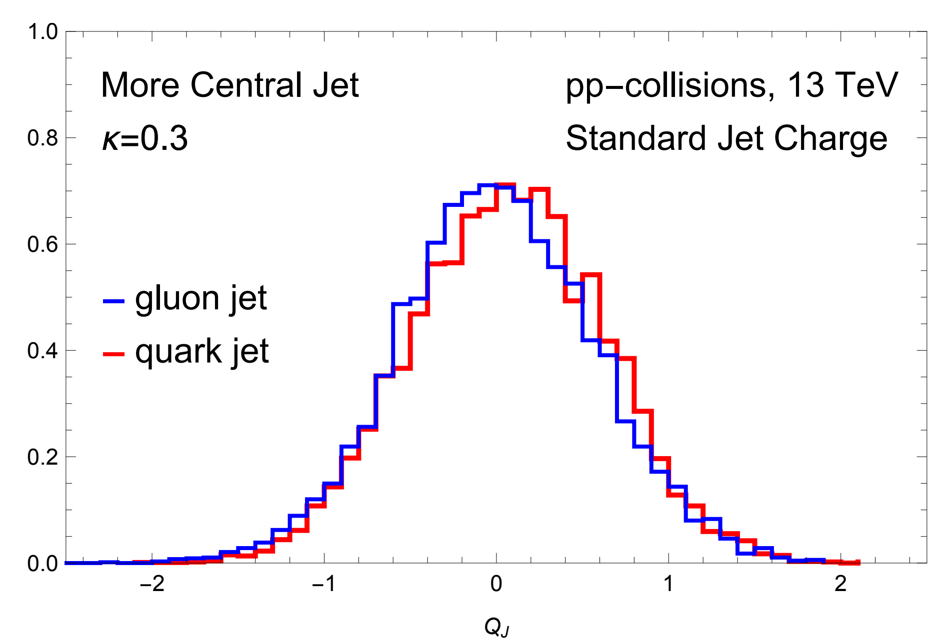

Poor q vs. g discrimination

Dynamic Jet Charge

[Kang, Liu, SM, Spraker, Wilson (2021)]

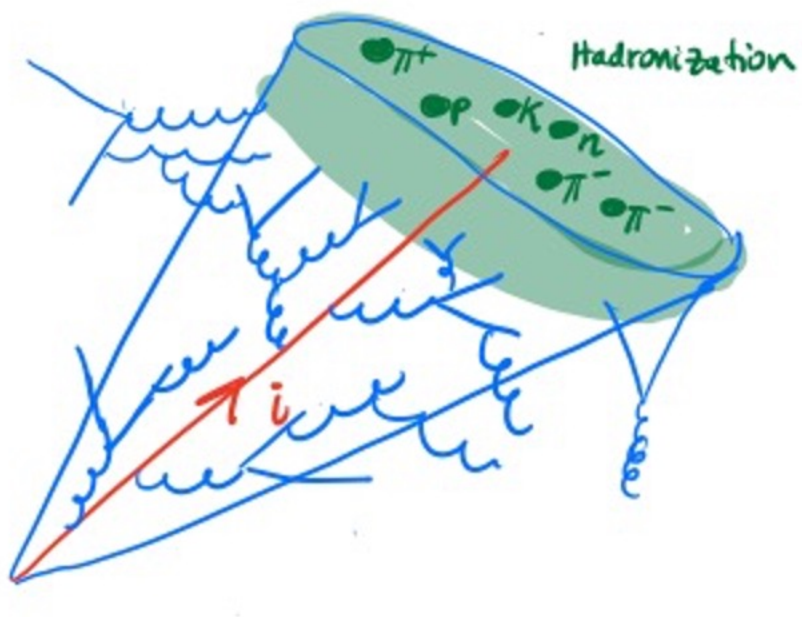

$$Q^i_{\rm dyn} = \sum_{h \in i\text{-jet}} z_h^{\kappa(z_h)}\, Q_h$$

$$\kappa(z_h) = \begin{cases} k_<, & z_h < \xi_{\rm cut} \\ k_>, & z_h \geq \xi_{\rm cut} \end{cases}$$

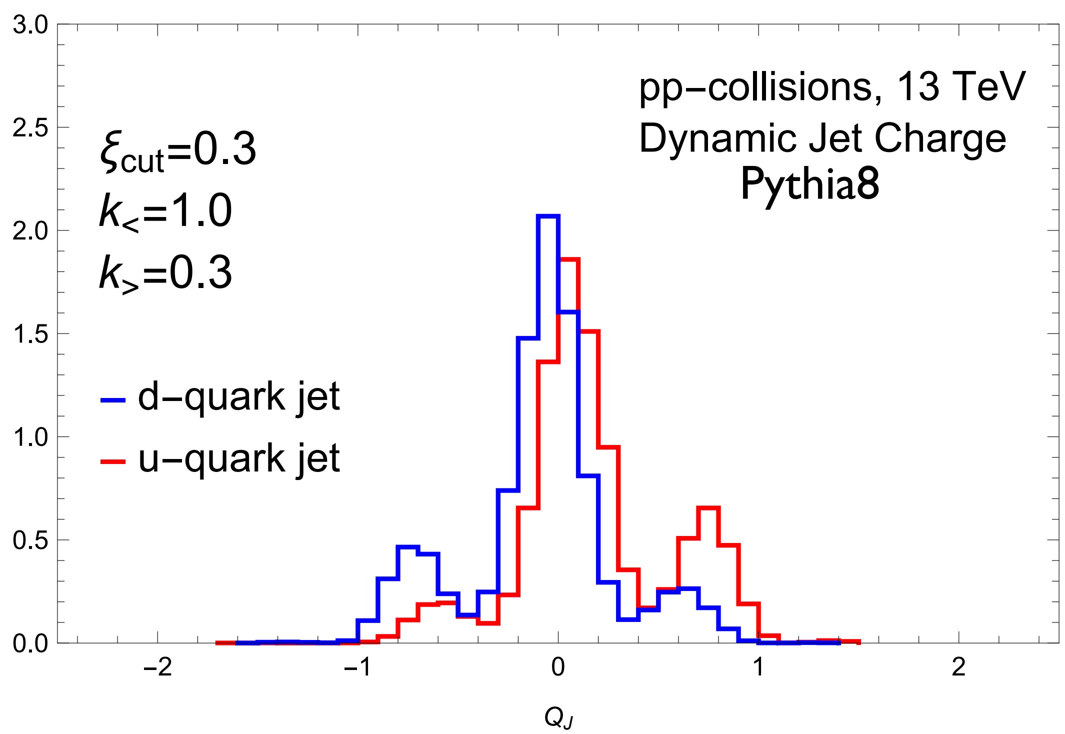

Good u vs. d discrimination

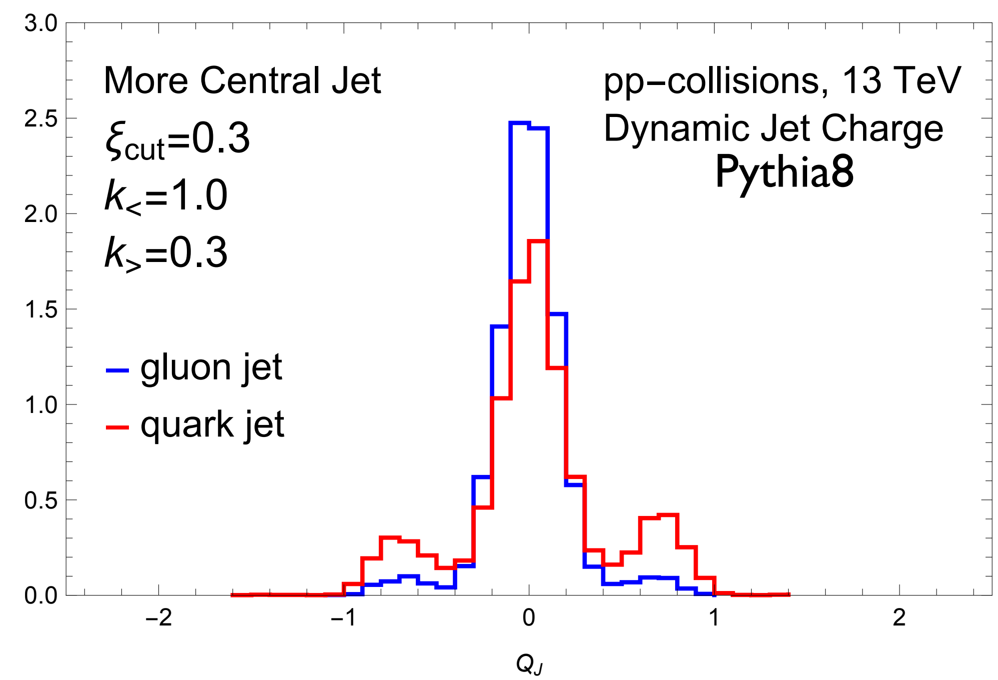

Decent q vs. g discrimination

Jet Charge ROC Curves

[Kang, Liu, SM, Spraker, Wilson (2021)]

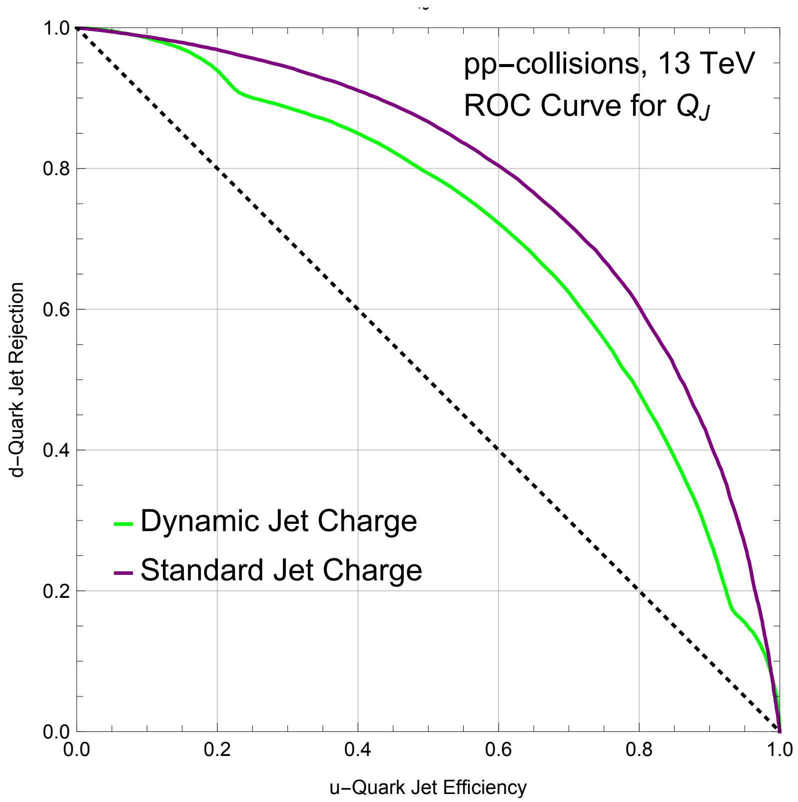

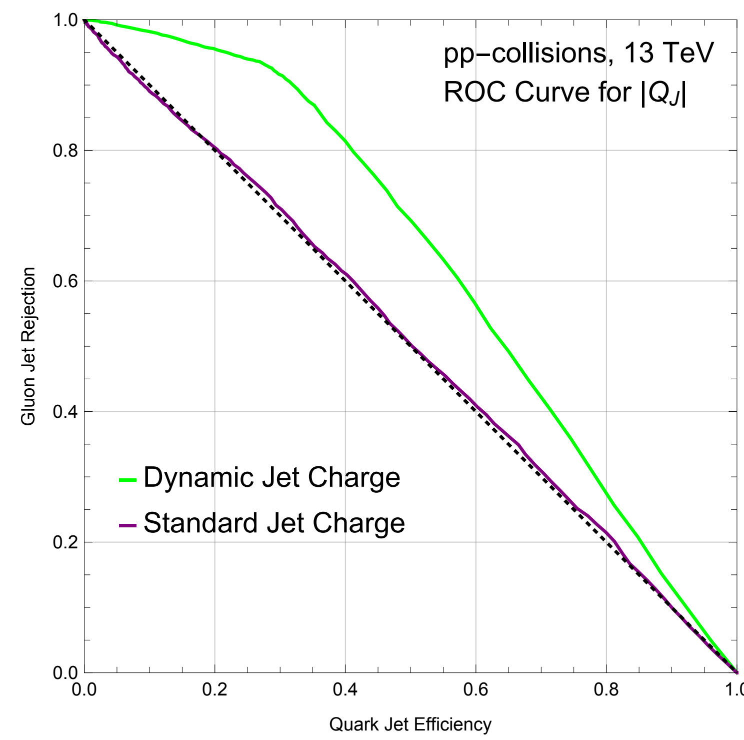

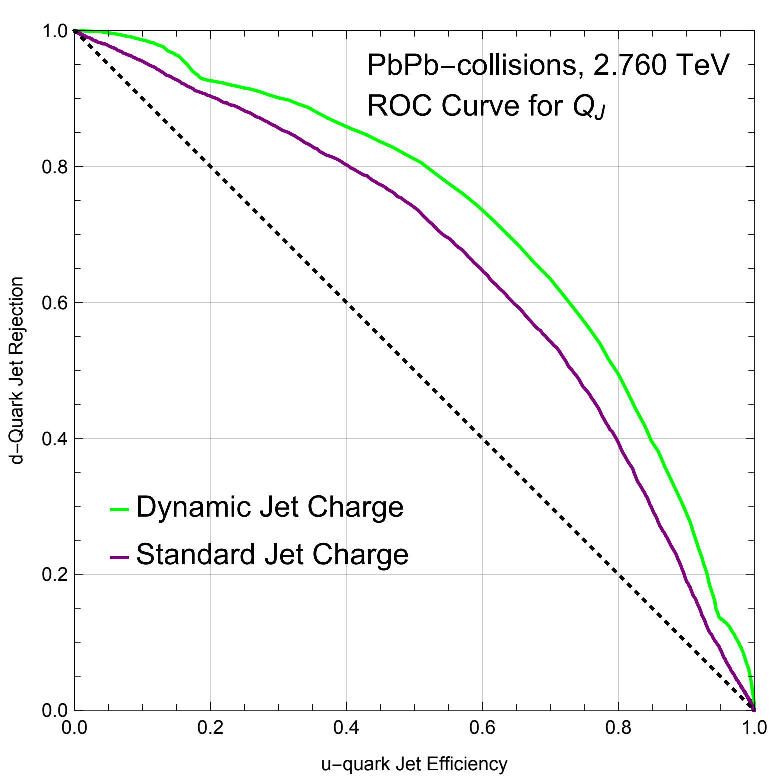

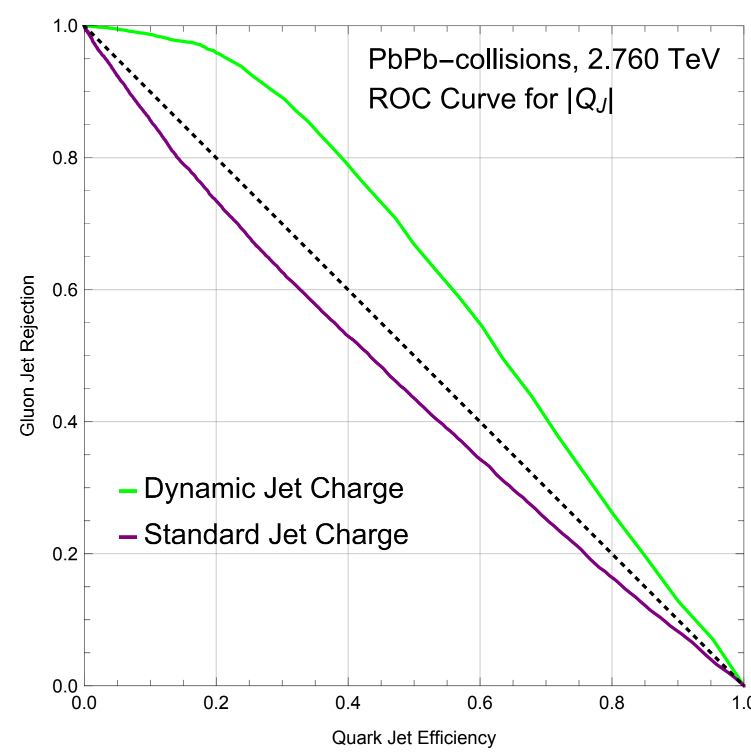

u vs. d discrimination

q vs. g discrimination

Jet Momentum Momentum Imbalance in DIS

[Collins, Soper, Sterman; Ji, Ma, Yuan; Liu, Ringer, Vogelsang; Arratia, Kang, Prokudin, …]

$$q_T = |\vec{P}_{J_T} + \vec{P}_T^e| \ll P_T^e$$

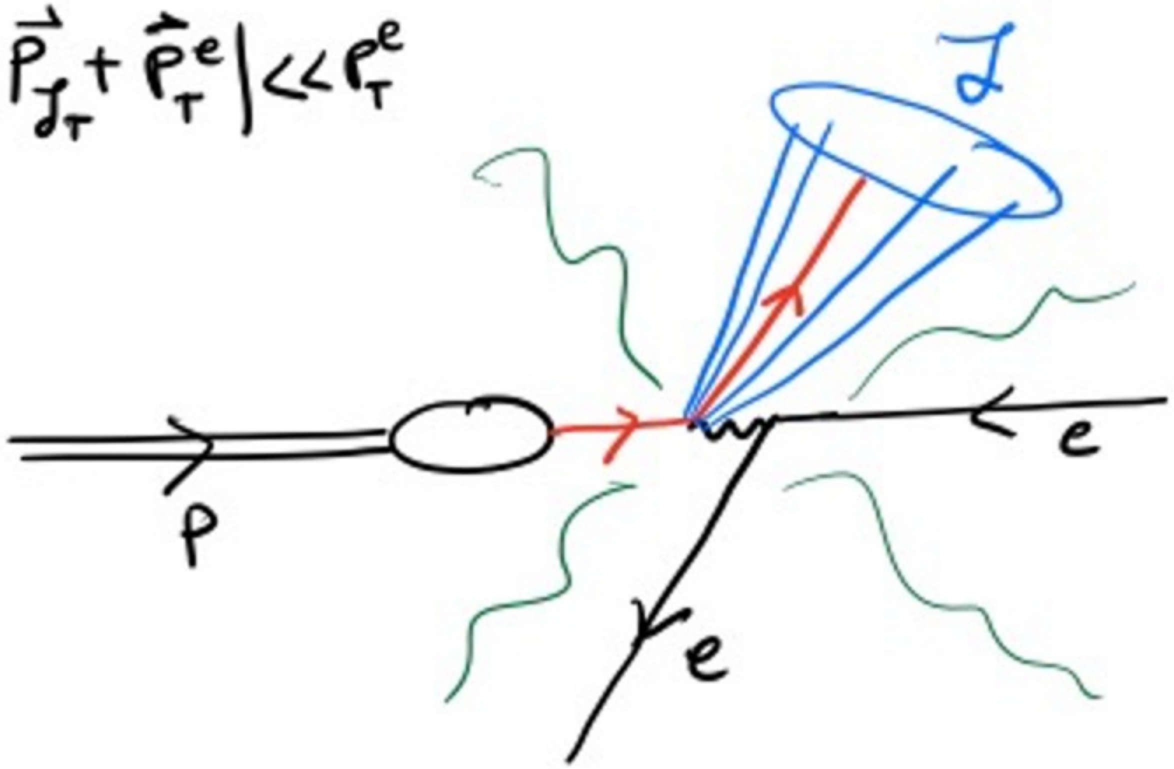

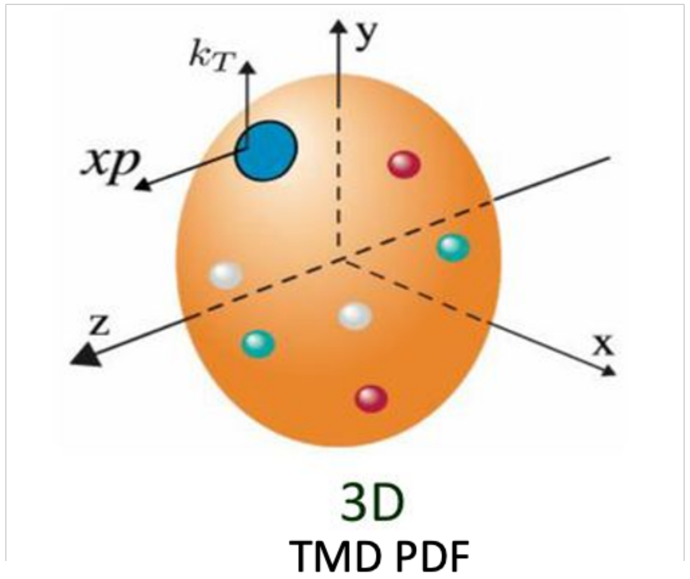

- TMD PDFs give a 3-dimensional view of the momentum distributions of partons in the proton

- This observable is sensitive to specific flavor combinations of TMDPDFs

$$d\sigma \sim \sum_i \tilde{f}_i(x, k_T) \otimes H \otimes S \otimes J_i$$

Jet Momentum Momentum Imbalance in DIS

[Kang, Liu, SM, Shao (2020)]

Measure the jet electric charge

$$q_T = |\vec{p}_{J_T} + \vec{p}_T^{\,e}| \ll p_T^e$$

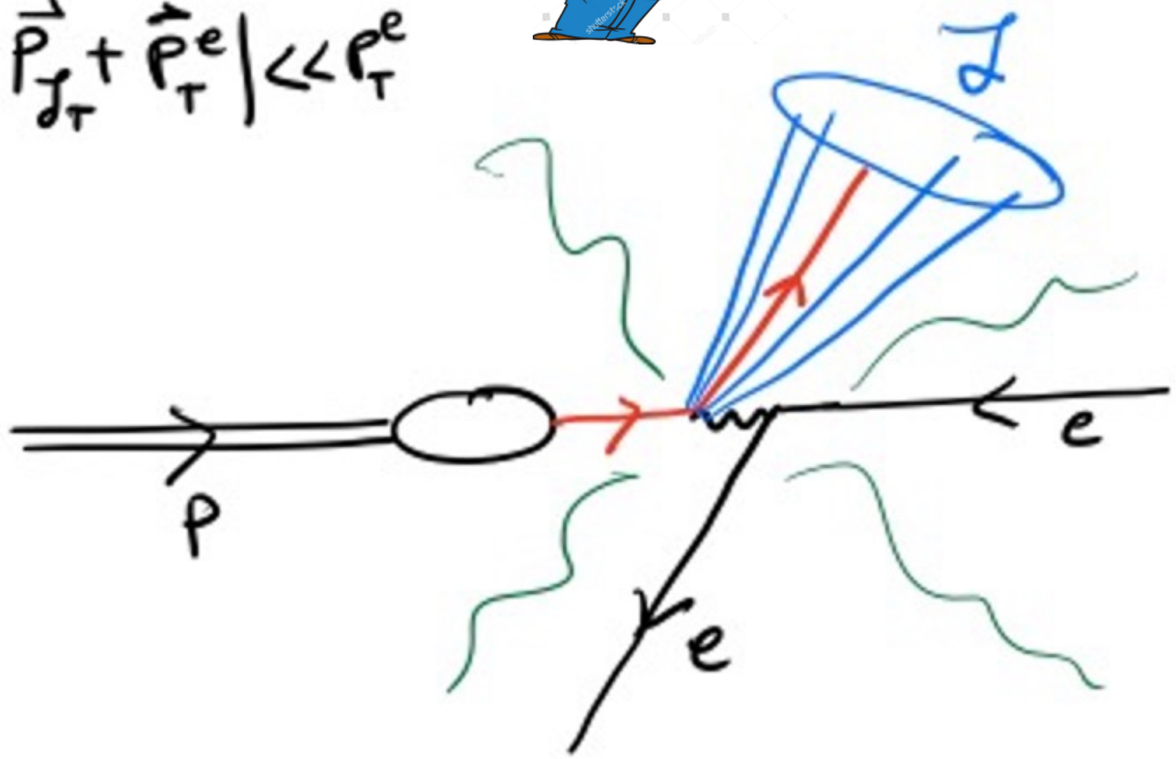

$$Q_\kappa^i = \sum_{h \in i\text{-jet}} z_h^\kappa \, Q_h$$

- This observable is sensitive to specific flavor combinations of TMDPDFs

$$d\sigma \sim \sum_i \tilde{f}_i(x, k_T) \otimes H \otimes S \otimes J_i$$

Jet Momentum Momentum Imbalance in DIS

[Kang, Liu, SM, Shao (2020)]

Measure the jet electric charge

$$q_T = |\vec{p}_{J_T} + \vec{p}_T^{\,e}| \ll p_T^e$$

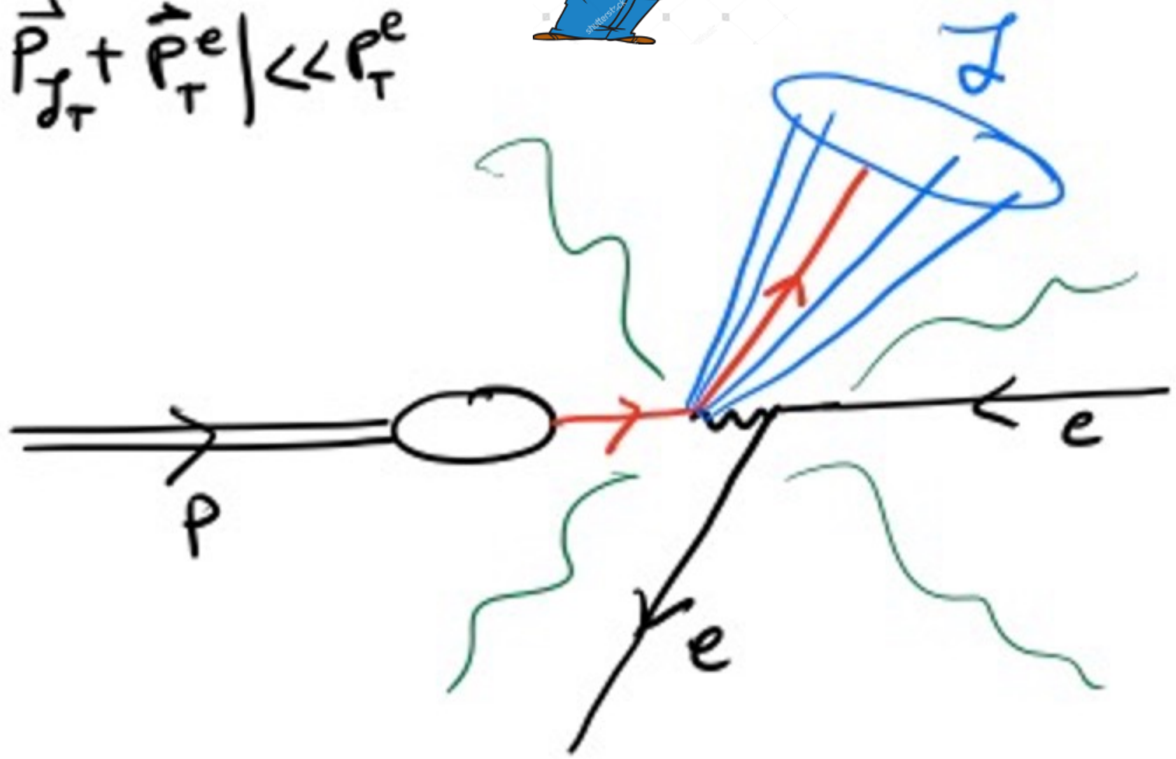

$$Q_\kappa^i = \sum_{h \in i\text{-jet}} z_h^\kappa \, Q_h$$

- This observable is sensitive to specific flavor combinations of TMDPDFs

$$d\sigma \sim \sum_i \tilde{f}_i(x, k_T) \otimes H \otimes S \otimes \mathcal{J}_i$$

Measure the jet electric charge

$$d\sigma \sim \sum_i \tilde{f}_i(x, k_T) \otimes H \otimes S \otimes \mathcal{G}_i(Q_J)$$

Unpolarized TMD Flavor Separation with Jet Charge

[Kang, Liu, SM, Shao (2020)]

$q_T = |\vec{P}_{J_T} + \vec{P}_T^e| \ll P_T^e$

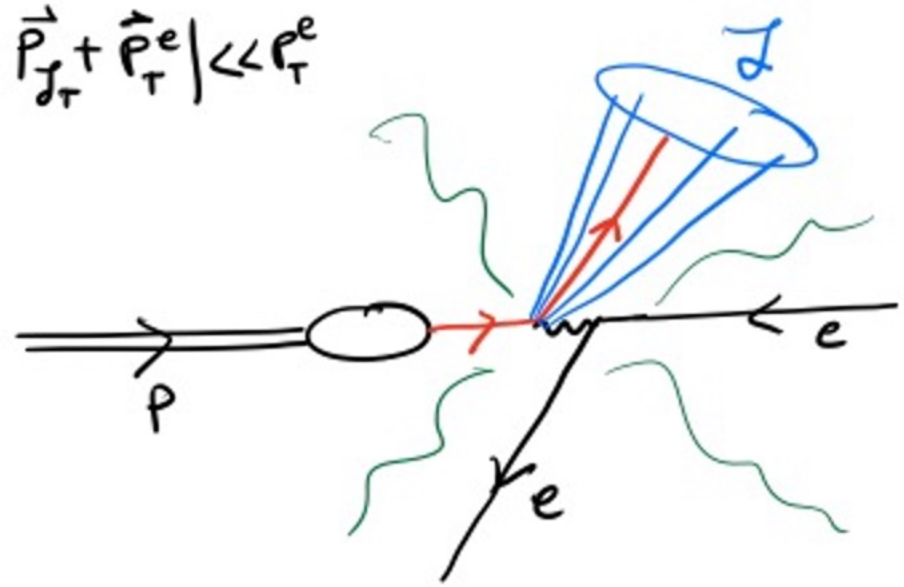

$$d\sigma \sim \sum_i \tilde{f}_i(x, k_T) \otimes H \otimes S \otimes J_i$$

Measure the jet charge to separate quark flavors

$$d\sigma \sim \sum_i \tilde{f}_i(x, k_T) \otimes H \otimes S \otimes G_i(q_J)$$

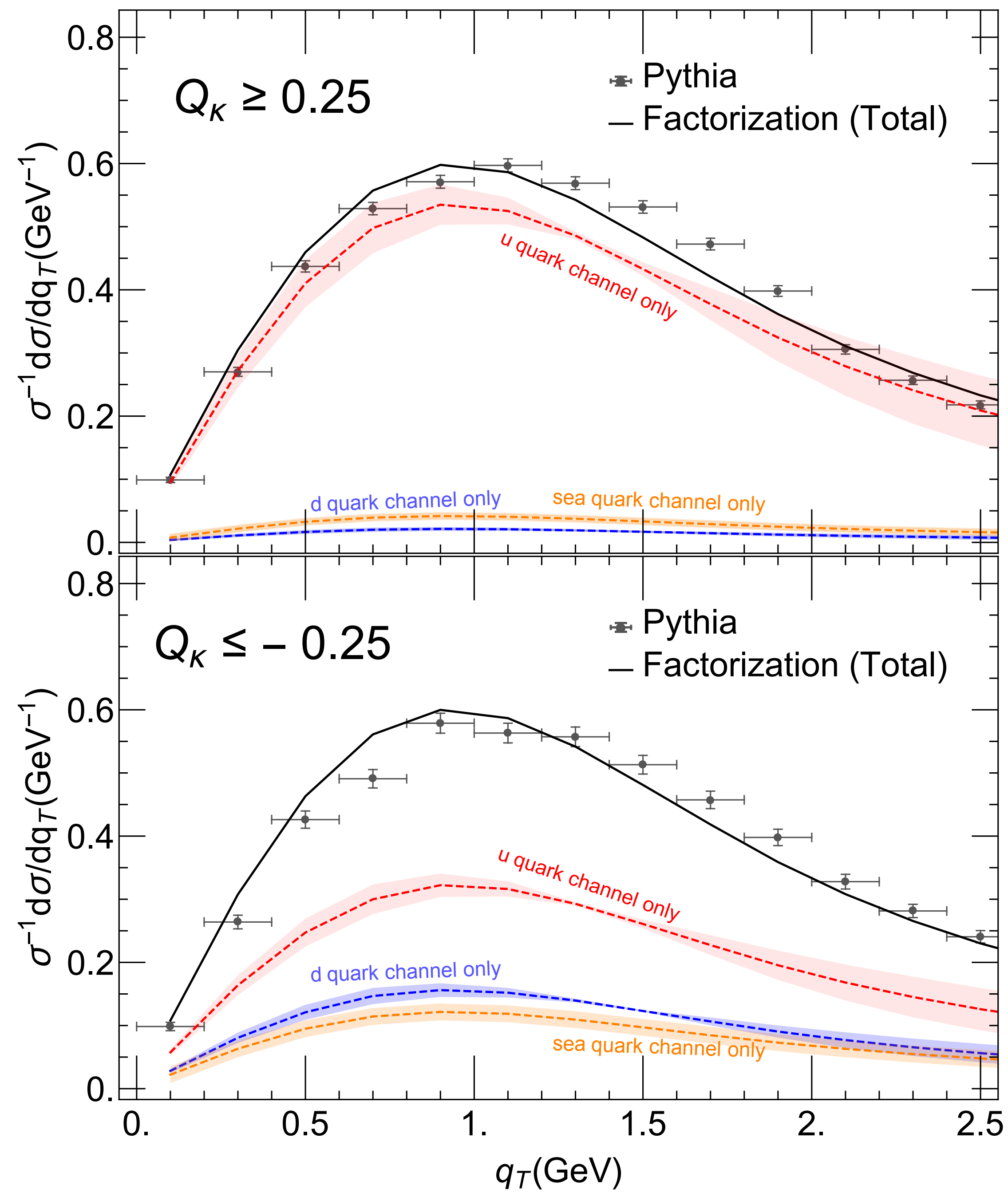

FIG. 2. The relative size of contributions from the unpolarized u-, d-, and sea quark TMDs.

Polarized TMD Flavor Separation with Jet Charge

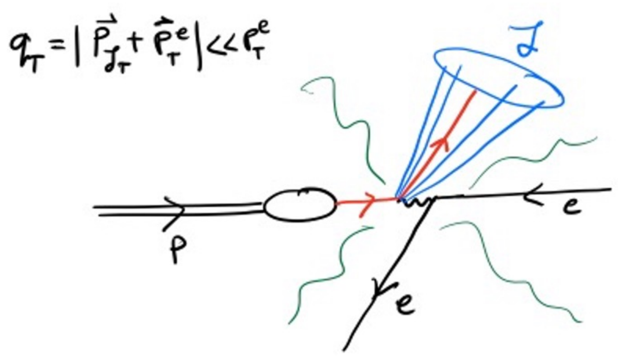

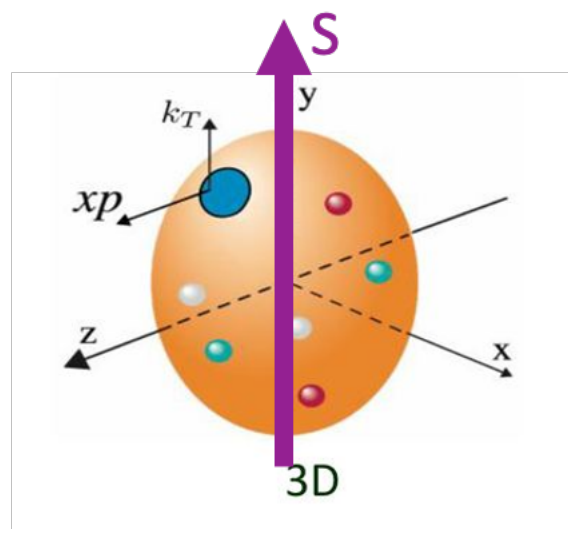

- Polarized TMD PDFs probe correlations between proton spin and 3D momentum distributions of partons in the proton and can be accessed via the asymmetry.

$$A_{UT} = \frac{\mathrm{d}\sigma(S_\perp^\uparrow) - \mathrm{d}\sigma(S_\perp^\downarrow)}{\mathrm{d}\sigma(S_\perp^\uparrow) + \mathrm{d}\sigma(S_\perp^\downarrow)}$$

[Kang, Liu, SM, Shao (2020)]

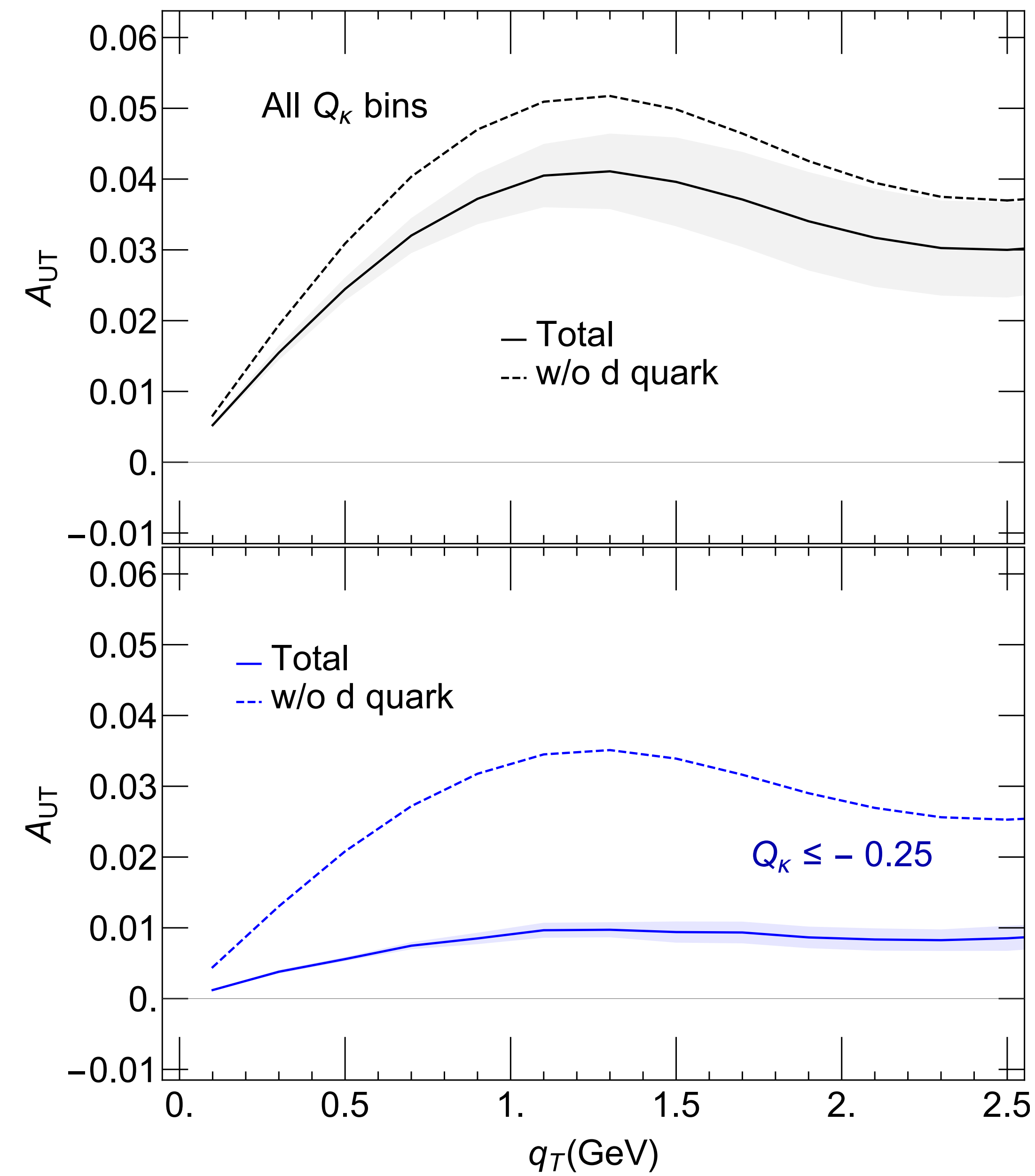

FIG. 4. Sensitivities of the d-quark channels to the Sivers asymmetry.

Electroweak Physics at the EIC

- The EIC is primarily a QCD machine.

- However, electroweak physics at the EIC can play an important role for:

- constraining new physics via precision measurements of electroweak couplings
- SMEFT Analyses
- electroweak probes of nucleon spin structure (NC, CC DIS)
- Jet electric charge probe

- This is facilitated by:

-high luminosity
-wide kinematic range
-polarized beams
-range of nuclear targets